Anadolu Psikiyatri Dergisi || ISSN: 1302-6631 || Volume 25; Number 5
https://doi.org/10.5281/zenodo.13842690

NEUROSEGNET: A PANOPTIC SEGMENTATION METHOD BASED ON DEEP LEARNING AND BIG DATA PROCESSING FOR THE IDENTIFICATION OF SPECIFIC NEUROLOGICAL CONDITIONS

[1]Ms.Srilakshmi CH, [2]Dr.K.Balasubadra

[1] Assistant Professor, R.M.D. Engineering College, Tamil Nadu, India
[2] Professor, R.M.D. Engineering College, Tamil Nadu, India

Abstract

Our work's main goal is to render a deep panoptic segmentation model specifically for medical image analysis, with an emphasis on recognizing common neurological disorders. Our model seeks to precisely identify and categorize various regions in brain scans through the integration of sophisticated segmentation technique with Autoencoder based deep Neural Network, thereby aiding in the identification and diagnosis of Neurodegenerative neurological disorders. This method could lead to more successful patient outcomes in neurological healthcare by increasing the accuracy of medical image interpretation. The proposed methodology is geared towards furnishing precise and efficient automated detection and segmentation of neurological irregularities, encompassing lesions, in medical imagery using brain scan images. This innovative approach holds significant promise in revolutionizing the landscape of medical image analysis, offering valuable support to healthcare practitioners in their diagnostic and therapeutic undertakings in web-based form for neurological disorders. The proposed model is designed to support healthcare diagnosis by providing a reliable and effective system that enables automatic recognition and categorization of neurological disorders using imaging techniques of the brain. By leveraging specially designed U-NeuroSegNet infused with big data Spark processing, we achieved exceptional accuracy and efficiency in identifying neurological abnormalities. In the proposed NeuroSegNet, the work focuses to contribute significantly to advancements in neuro-oncology and personalized patient care, ultimately benefiting individuals affected by neurological disorders. Our study utilized big datasets consisting of brain scan images. Our NeuroSegNet model achieved F1-score of 95.6%, a high accuracy of 98.2%, precision of 97.8%, sensitivity of 93.7% and recall rate of 98.0. These results demonstrate the NeuroSegNet models effectiveness in accurately detecting Neurological disorders, lesions and tumors.

Keywords: U-NeuroSegNet, Panoptic Segmentation, NIWatershed Algorithm, Intersection over Union, Accurate Boundary Detection, Neorological Disorders.

1. INTRODUCTION

The work revolves around the implementation of panoptic instance segmentation for automated analysis of medical images, particularly focusing on neurological conditions using brain scans. Our work comprises a trained deep learning model to identify and precisely delineate neurological anomalies, and lesions. The model is designed to provide real-time results, enabling healthcare professionals to make faster and more accurate diagnoses. Dataset was taken from Kaggle public dataset and Chennai Brain and Spine Centre. In the context of our work, we employ deep learning algorithms, notably an enhanced and modified UNet, to scrutinize medical images and discern patterns indicative of various brain abnormalities. Conventional manual examination of medical images is laborious and susceptible to human error. In response to these challenges, we propose panoptic segmentation model suitable for brain scans based on modified UNet, a deep learning methodology, to automate and enhance the accuracy of identifying and segmenting neurological abnormalities using brain scans.

2. BASIC CONCEPTS

The work done in this research underscores the paramount significance of precise and efficient medical image analysis within the domain of neurology. Neurological disorders, such as lesions,necessitate prompt diagnosis and meticulous delineation to facilitate effective treatment planning. Conventional

manual examination of medical images is laborious and susceptible to human error. In response to these challenges, we propose employing panoptic segmentation based on U-NeuroSegNet, a deep learning methodology, to automate and enhance the accuracy of identifying and segmenting neurological abnormalities using brain scans.

This research endeavor holds immense potential for substantially elevating the standard of care provided to patients grappling with neurological conditions. The initial exposition of this kind of endeavor accentuates the critical and meticulous role medical imagery plays in the sphere of neurology. Conditions affecting the nervous system, within the brain demand swift and precise diagnosis to inform and gain insights on effective treatment strategies.

In response to these challenges, we advocate for the adaptation of a DNN-based panoptic segmentation technique, leveraging the power of deep learning infused with Apache spark big data processing framework to automate and refine the process of identifying and delineating neurological anomalies present in brain scans.This innovative research initiative holds the promise of significantly augmenting the caliber of healthcare services rendered to individuals afflicted with neurological disorders.

Our NeuroNet can detect the following Anold Chiari malformation, Arachnoid Cyst, Cerebellah Hypoplasia, Cisterna Magna, Colphocephaly, Encephalocele, Holoprosencephaly, Hydracenphaly, Moderate Ventriculomegaly, Intracranial hemorrhage, Severe Ventriculomegaly and Polencephaly.

Table -1: The Neurodegenerative Disorders addressed in this work along with description

Neurodegenerative Disorders	Description
Anold Chiari malformation	Anold Chiari malformation occur when brain tissues are pressed down to spinal cord due to skull being small at one side. This affects neuromuscular function.
Arachnoid Cyst	Archnoid cysts are fluid-filled growths in the brain and spinal cord that, when they enlarge beyond 3cm or bleed internally, result in permanent damage to nerves.
Cerebellah Hypoplasia	Cerebellar hypoplasia is a congenital problem when cerebellum is small in size. Less than the 10th percentile of gestational age for cerebellar diameter is considered harmful. For instance, the average TPD measurements range from 16.6 mm to 23.1 mm at 20.4 weeks of gestation and from 32.2 mm to 41.6 mm at 31weeks of gestation.
Cisterna Magna	Enlarged cerebellar region causes cisterna magna. It is a space in the posterior fossa dorsal to the medulla and caudal that is filled with cerebrospinal fluid. When larger than 10mm, they are usually dangerous causing neurological issues.
Colphocephaly	Colpocephaly is an uncommon genetic disorder characterized by lateral ventricle enlargement in two brain cavities. It is a congenital abnormality that results in the posterior brain ventricles growing larger than 10cc.
Encephalocele	A condition known as encephalocele results in brain tissue growing outside of a skull due to bone defect or any opening in skull causing neurological disorders.
Holoprosencephaly	When the human brain by birth is not predominately partitioned appropriately as right and left hemispheres people suffer from Holoprosencephaly problem and it is identified only in later stages of life.
Hydracenphaly	Hydranencephaly is an uncommon congenital condition in which there is no cerebral hemisphere.
Intracranial hemorrhage	Intracranial Hemorrhage relate to bleeding within the intracranial vault of the brain.

Polencephaly	Porencephaly refers to the existence of cystic cavities inside the brain tissue.
Ventriculomegaly	Ventriculomegaly is a disorder where a build-up of cerebrospinal fluid (CSF) causes the brain to enlarge. Ventriculomegaly is categorized into mild, moderate, and severe based on the degree of enlargement. Specifically, mild ventriculomegaly is defined as having a measurement of 10 to 12 mm, while moderate and severe ventriculomegaly are defined as having measurements of 12 to15 mm and greater than 15 mm, respectively.

3. Related Work

A novel CNN model was developed for object identification and word segmentation for medical image analysis is presented in (Yang et al 2023) for the identification and mapping of diseases' locations and regions are crucial for precise diagnosis. Authors (Elyan et al 2023) delved into the utilization of computing and its practicality in medical advancements. Employing computer vision and machine learning, extensive analysis was carried out for medical image analysis.

The use of artificial intelligence and advanced neural networks in medical imaging was explored by (Xuxin Chen et al 2022), probably offering a detailed summary of the subject. Meanwhile, Yu et al. (2023) concentrated on contrasting convolutional neural networks (CNNs) and their application in various medical diagnostic tasks.

In the work done by (Jianguo Chen et al 2023, Jianguo Chen and colleagues, 2023) addressed a new method for enhancing the adaptability of deep learning models for analyzing medical images. Their system, which consists of a collection of deep learning model parts and elements designed for specific tasks, might simplify the creation and modification of AI models for different medical imaging activities. This could lead to more customized answers and quicker adjustments to particular diagnostic requirements.

In 2021, Zhou and colleagues (Zhou. J et al 2021) introduced E-Res U-Net for image segmentation, this model improved the accuracy of the model using ultrasonic muscle images. This model's structure was altered from the basic U-Net to enhance performance in three aspects, the dilated convolution component, the E-Res layer, and the E-Res.

(Qian et al 2023) suggested a brand-new density-regression-based multi-scale convolutional UNet (MSCA-UNet), and when they compared it with other sophisticated density regression techniques, they revealed two significant advances. one is the encoder component, for which they used an MSCA (Multi-scale Contextual Attention) block with multi-scale interaction capabilities.

A dual-attention based dense R-CNN model was presented by (Veta et al 2022). In this work involved a versatile and all-purpose instance segmentation framework Mask R-CNN. It can recognize objects in the image with good level of accuracy and produce superior segmentation labels for each occurrence.

In order to determine the performance of the designed CNN (Yuadi et al 2023) used AUC which tells how well the model can distinguish between classes across several thresholds. They showed area under curve, assesses the accuracy of segmented regions comparing with ground truth,and showed how superficial it is compared to pixel accuracy.

In order to control side-effects of over-segmentation (Sharma. A.K et al 2024) developed a neural network model which only retained only the minimum value of the objective area plus the the required edges of the object identified was safeguarded while the MRI image was being filtered and denoised

The 3D UNet architecture proposed by (Hwang et al 2023) shows great potential as a volumetric segmentation tool, especially when applied to brain scans. It is possible to capture spatial information throughout the entire volume of the brain scans by extending the U-Net architecture into three dimensions. This is an important development for precise segmentation.

The work done by (Bhanothu et al 2020) focused on the automatic classification of brain abnormalties using a Intergation of VGG-16 NN technique with Fast R-CNN algorithm Fast R-CNN is an improvement over the original R-CNN method, designed for faster and more accurate object detection. It involves two main stages: generating region proposals and then classifying these proposals using a deep learning network.

Incorporating uncertainty quantification helps in understanding the reliability of the model's predictions. This is crucial in medical imaging (Kim et al 2018), where decisions based on automated segmentation need to account for potential variability and errors. Kim et al. (2018) proposed a framework which focused on segmenting brain abnormities and other quantifying uncertainties in biomedical images, which is particularly useful for conditions like traumatic brain injuries, stroke, multiple sclerosis.

(Ramtekkar et al., 2022) used whole brain imaging and a gray level confrontation matrix to build a deep k-means fuzzy CNN for the detection of glioma in brain scan images.

4. U-NeuroSegNet based System for Identifying Neurological Disorders Methodology

A Spark based DNN Model, U-NeuroSegNet Architecture was specially designed and for segmentation a modified Neuro-Intrinsic Watershed algorithm was utilized for the work done. In our work U-NeuroSegNet When the neural network is fed with brain images as inputs, it classifies images by instances and identifies several classes of neurological abnormalities. The U-NeuroSegNet extracts relevant features from the input image, and then projects them into segmentation masks. Spark is a data processing framework used for big data workloads which processes huge data sets using cluster computing.Spark Framework supports machine learning and big data processing in its engine.

Using panoptic segmentation, which combines instance and semantic segmentation, we created a unique U-NeuroSegNet to capture intricacy pixel by pixel. Our U-NeuroSegNet module focuses on tailoring the architecture to suit the specific need to discover abnormal neurological conditions like Anold Chiari malformation, Arachnoid Cyst, Cerebellah Hypoplasia, Cisterna Magna Colphocephaly, Encephalocele, Holoprosencephaly, Hydracenphaly, Moderate ventriculomegaly, Intracranial hemorrhage, Severe ventriculomegaly and Polencephaly.

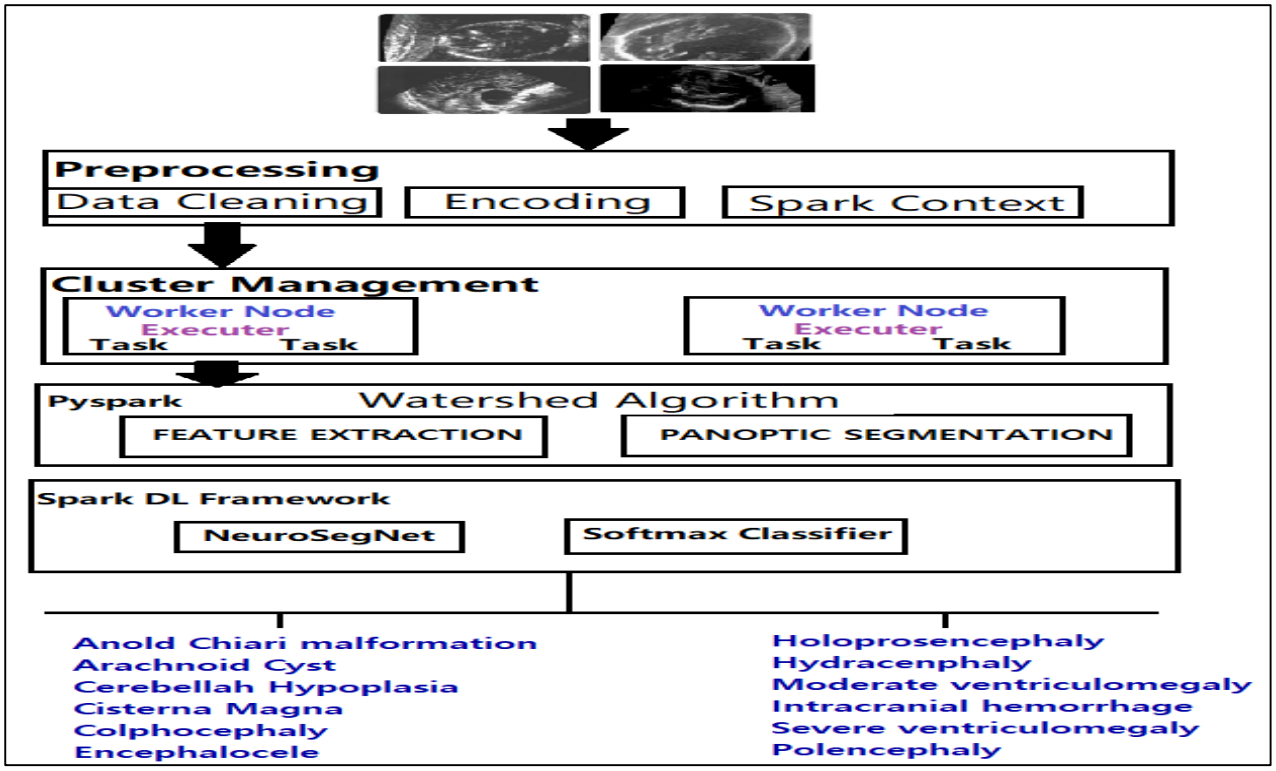

Figure 1 - Big data Based Apache Spark for NeuroSegNet

Our model utilized Apache Spark IDE for processing. In the Spark framework we utilized ApacheMxNet,it is a module in the framework that supports machine and deep learning processing. Automatic scaling is supported by multiple GPU servers and multi-node clusters. NVIDIA Spark framework supports accelerated computing, through RAPIDS component to support pipeline processing.

4.1 Neuro-Intrinsic Watershed Algorithm

The modified Neuro-Intrinsic watershed algorithm is a technique used for image segmentation, particularly for separating overlapping objects or regions. In our project, the Neuro-Intrinsic Watershed algorithm is utilized to segment the brain images into individual regions or components, facilitating the identification and analysis of distinct anatomical structures and pathological abnormalities. Specifically, the Neuro-Intrinsic Watershed Algorithm has been utilized to address challenges such as heterogeneity and irregular shape, which can complicate traditional segmentation approaches. By applying the algorithm to preprocessed brain scan images, we were able to effectively partition the regions, enabling precise measurements of volume and facilitating quantitative analysis of abnormalities.

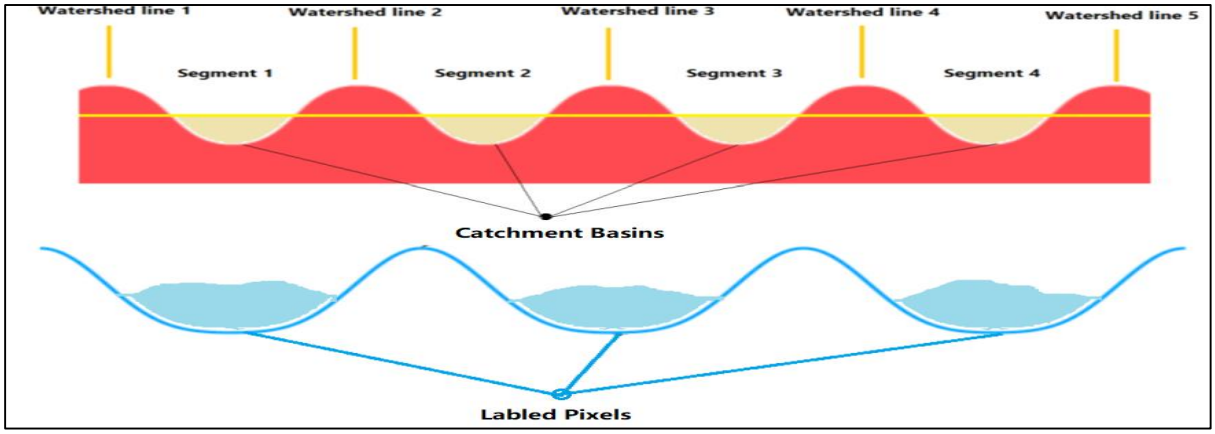

Figure 2- Watershed basins

Our Neuro-Intrinsic watershed algorithm is a variation of classical Watershed algorithm for segmenting brain scan images. The algorithm treats pixel intensities as a terrain, where higher intensities represent peaks and lower intensities represent valleys. The algorithm then "floods" the map from the valleys (pixels with the lowest intensities) and lets the watershed markers converge at the peaks (pixels with the highest intensities). If refinement of bounding regions are necessary NIWatershed algorithm auto adjusts the bounds. Once the U-NeuroSegNet predicts potential bounding boxes for objects in an image, the NIWatershed algorithm can be applied to better separate objects that are close together or overlapping conveniently that helps in increasing accuracy effectively.

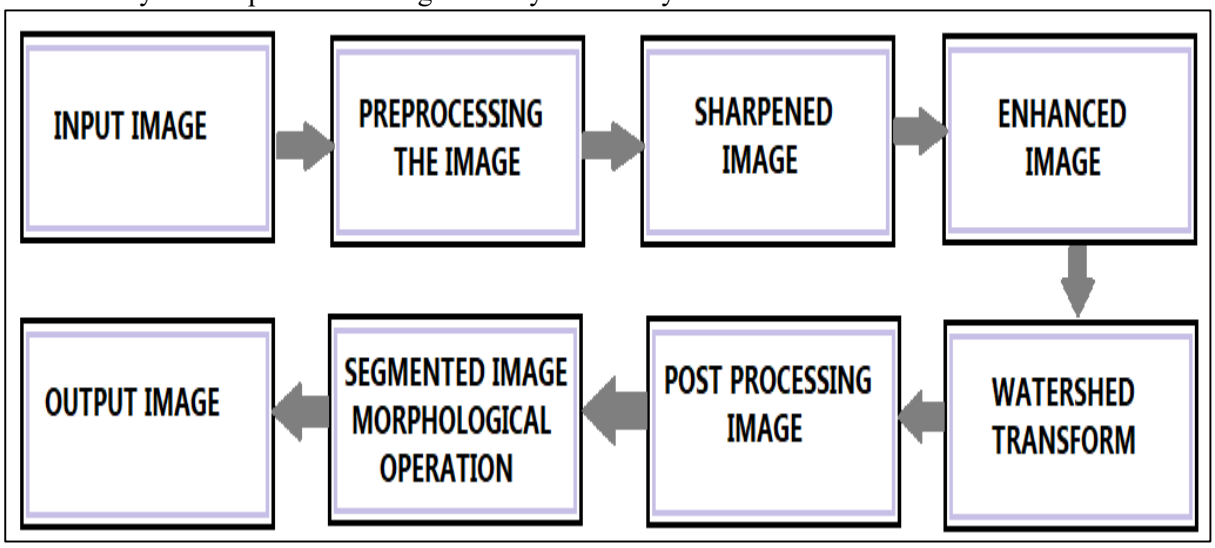

Figure 3 - Neuro-Intrinsic Watershed processing

NIWWatershed Segmentation works by grouping pixels based on similar intensities, it separates the abnormal region from rest of normal region of brain scan image. The NIWWatershed Segmentation is a morphological operation to double check the predicted output.

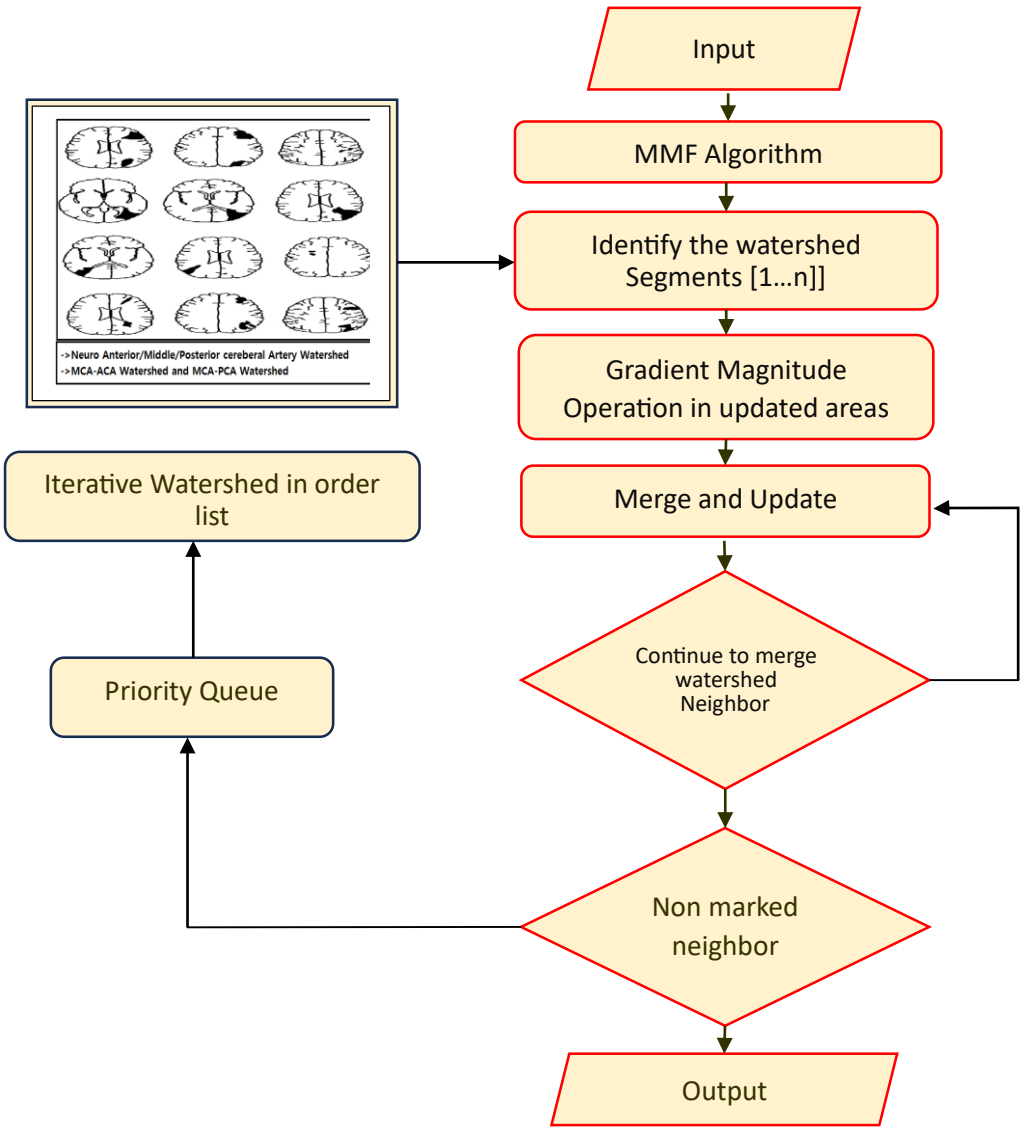

Figure 4 - Neuro-intrinsic Watershed Algorithm processing

Pseudocode for NIWatershed Segmentation

Input: Brain image *Im*
Output: Segmented regions *Sr*

Begin

1. Preprocess the image:

a. Convert image I to grayscale

Im_gray(x, y) = I(x, y)

b. Apply Gaussian smoothing to reduce noise

Im_smooth(x, y) = $\sum_{i=ks}\sum_{j=-ks}$ $G_k(i, j)$ * Im_gray(x+i, y+j)

where $G_k(i , j)$ is the Gaussian kernel, & k_s is the kernel size.

2. Enhance features:

a. Use histogram equalization to improve contrast

Im_eq(x, y) = [(Im_gray(x, y) - min(Im_gray)] / [(max(Im_gray) - min(Im_gray)]

3. Compute the gradient magnitude:

a. Compute gradients in x and y directions using Sobel filters

Im_gray = $\partial I_e q(x, y) / \partial x_d$

$G_k y(x_d, y_d) = \partial I_e q(x, y) / \partial y_d$

b. Compute gradient magnitude image

$G_k(x_m, y_m) = sqrt(G_k x(x, y)^2 + G_k y(x, y)^2)$

4. Compute the distance transform:

a. Apply distance transform to the gradient magnitude image to get the distance map

$D_m(x, y) = max_{dist} – nearest\_edge_{dist}(x, y)$

where max_dist is the maximum distance from any pixel to the nearest edge.

5. Create markers for the watershed algorithm:

a. Use region-growing or machine learning techniques to identify markers

Markers = [$M_i | M_i$ = (x, y) where $Im_e^q(x, y)$ > threshold]

b. Optionally, create background markers

BackgroundMarkers = [B_j | B_j = (x, y) where $Im_e^q(x, y)$ < threshold]

6. Application of NIWatershed transformation:

a. Initialize the watershed algorithm with the markers

WatershedMarkers = Markers ∪ BackgroundMarkers

b. Use the gradient magnitude image for segmentation

- Initialize a flooding process from markers
- For each marker, "flood" into neighbouring pixels based on gradient magnitude.
- Update labels based on the watershed lines formed by gradients.
- The watershed lines are boundaries where the gradient magnitude is high.

7. Postprocess the segmented image:

a. Smooth boundaries and remove small objects

- Apply morphological operations such as dilation and erosion

Sr_morph(x, y) = (Erosion or Dilation of Segmented Image Sr)

b. Optionally refine segmentation results using additional techniques or manual corrections.

8. Output the segmented image Sr with highlighted regions of interest.

End

4.2 Panoptic Segmentation

A comprehensive strategy that combines instance and semantic segmentation referred to as panoptic segmentation. Semantic segmentation offers an in-depth knowledge of the discrete characteristics found in brain images, while instance segmentation assigns a distinct label to each pixel. Object detection and segmentation are merged into a single, cohesive framework through panoptic segmentation. With this technique, regions of interest are identified using the output of an object detector, and object boundaries are then precisely delineated using a segmentation module.

4.2.1 IoU & ABD in Panoptic Segmentation

Our model NeuroSegNet uses panoptic segmentation. The two most important factors affecting panoptic segmentation are Intersection over Union and Accurate Boundary Detection. By finding the difference between overlapped predicted bounding box and the ground truth bounding box, the crucial metric intersection over union evaluates how well the predicted segmentation matches the actual object boundaries. The confidence score over the projected bounding box and predicted object class is directly impacted by the intersection over union. A modified edge detection technique is used for Accurate Boundary Detection [ABD] in order to predict boundaries with high precision.

4.2.2 Panoptic Segmentation is dependent on ground truth

For complex tasks of Panoptic segmentation, it requires a solid Ground Truth data. The training images have been accurately annotated to indicate the exact boundaries of objects. The model uses this for testing its output predictions against the ground truths to decide and improve accuracy.Panoptic segmentation uses Gaussian filters with Laplacian transformation for edge detection. The Gaussian filters are used to smooth out the noise and the Laplace function is used to depict the edge boundaries clearly as shown in equation(1).

$$\mathbf{GoL_{normalized}(x,y)=\sigma 2 \cdot LoG(x,y)=1/\sqrt{\prod \sigma 2(x^2+y^2 2\sigma^2-1)e-x^2+y^2 2\sigma^2}} \quad \textbf{- Eqn(1)}$$

In our modified Panoptic segmentation, the nearest local density maximum function is used to represent pixel in high dimensional space.

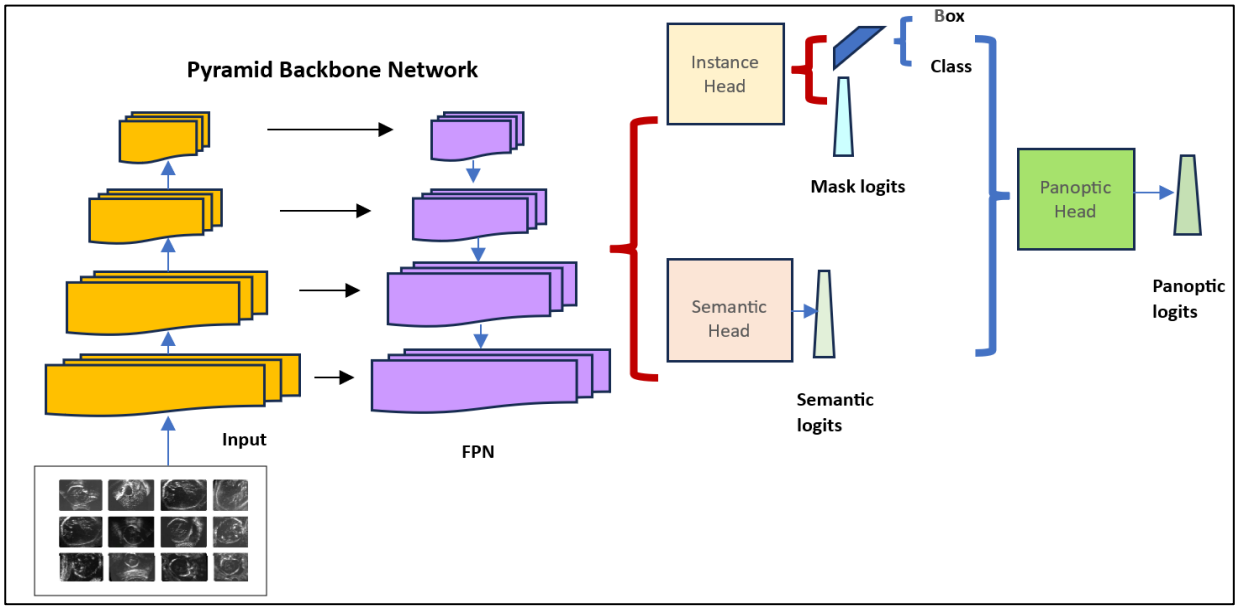

Figure 5 – Neuro Intensive lightweight Panoptic Segmentation

4.3 U-NeuroSegNet Encoder / Decoder

The U-NeuroSegNet comprises an encoder-decoder network structure augmented with skip connections, which play a vital role in preserving spatial information throughout the segmentation process. In our proposed U-NeuroSegNet is based on the principle of encoding and decoding process The encoder in our U-NeuroSegNet extracts detailed features from the input medical image, capturing relevant patterns indicative of abnormalities presence. Subsequently, the decoder reconstructs the segmented output, utilizing the extracted features to delineate boundaries accurately. While no specific formula governs this process, the architecture's design incorporates principles related to convolutional operations, skip connections, and activation functions to facilitate effective brain segmentation. The U-NeuroSegNet architecture, when carefully configured, can effectively delineate regions in medical images, contributing to improved diagnostic accuracy and more precise treatment planning in clinical settings.

The architecture and parameters of the neural network model are configured for image segmentation tasks by the U-NeuroSegNet configuration module. This module ensures that the U-NeuroSegNet model is appropriately configured to effectively segment brain images and extract relevant features for classification.

4.3.1 Subnet Division

Subnet division involves dividing the neural network architecture into smaller, manageable subnetworks. In our model we divide the neural network into multiple subnetworks to facilitate parallel processing and optimize computational efficiency.

4.3.2 Category Brain Slicing

This method focuses on segmenting the brain into different categories or regions based on specific criteria. In our work, categorically brain slicing is used to partition the brain images into distinct regions corresponding to different anatomical structures and pathological features, aiding in the accurate detection and classification of brain images.

4.3.3 Narrow Object Region

Narrow object region detection aims to identify and delineate small or thin structures within the images. In our work done, this method is employed to detect narrow regions within the brain images that correspond to abnormality boundaries or blood vessels, enabling precise segmentation and analysis.

The reason why encoder and decoders are relevant to our specially designed DeepU-NeuroSegNet is because output results must have the same dimension as the input. In the Panoptic Segmentation task done ensures output image is of same dimension as the original input.Our DeepU-NeuroSegNet uses a modified panoptic segmentation that is suitable for ultrasound images. The neural network is fed brain scan images as inputs, and classifies objects pixel by pixel.

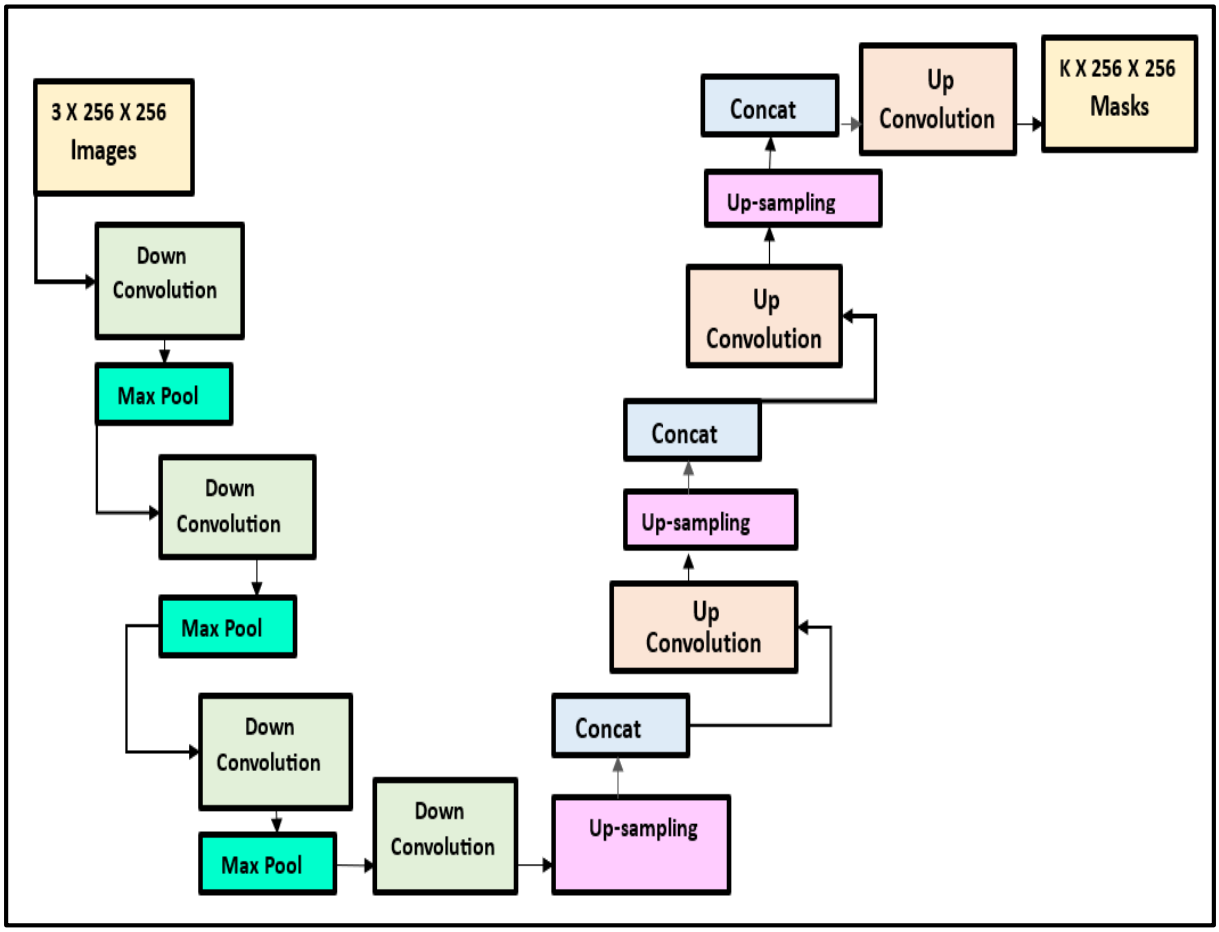

Figure 6 - U-NeuroSegNet Architecture

In the encoder-decoder architecture all pixels are classified as abnormal/normal. The encoder takes the required features from images. The encoder contains conv layers, Relu and Maxpool to extract relevant features for each class. The decoder creates feature maps and takes the extracted vectors and reconstructs a segmentation mask. Skip Connection is added to decoder to ensure decoder works with specific features rather than general ones.

An loss intrinsic cross-entropy based loss function is used in the developed for our NeuroSegNet to compare the accuracy of each class output with the ground truth value. For every individual feature, the ground truth value grtruth(ќ) is compared to the predicted output ¸Ö for each of the n classes as shown in Equation (2)

$$\text{Loss}= -\sum_{k=1}^{n} grtruth(ќ) \circledcirc log \oplus (softmax((ϒ)ќ) \quad \text{- Eqn(2)}$$

$$softmax((ϒ)ќ = \frac{\sum_{k=1}^{i} Öќ}{\sum_{j=1}^{n} Öj} \quad \text{- Eqn(3)}$$

Equation (3) illustrates the softmax function, where the vector is denoted by ϒ. The exponential function of the input vector is represented in the numerator, while the sum of the exponential functions of the output vector is represented in the denominator. Our Deep Learning NeurologicalNet model differs from traditional CNN/DNN models in that it is neither fully connected nor linear in nature, providing a unique structure tailored for our specific application to diagnose various neurological conditions.

In our U-NeuroSegNet the dice loss as shown in equation(4) is a loss function that weighs the imbalance between the intersection area and total area in similar kind of images. The dice loss will be less when dice coefficient is high. Dice loss represents the imbalance in segmentation mask. The Ψ represents the smoothing factor and is used both in numerator and denominator

$$\text{Dice Loss}= 1-\frac{\mathbf{2\sum_{l=1}^{n} softmax((ϒ)\circledcirc ќ grtruth(ќ)+\Psi}}{\mathbf{\sum_{l=1}^{n} grtruth(ќ)\circledcirc softmax((ϒ)ќ+\Psi}} \quad \textbf{- Eqn(4)}$$

Our U-NeuroSegNet consists of left-hand-side contracting path and right-hand-side expansive path both paths function symmetrically this mapping structure leads to high accuracy to aid our computer assisted diagnosis. The left-hand-side path is designed using repeated application of unpadded 3x3 convolution layers, then rectified linear unit is applied, then maxpooling with 2x2 operation with stride1 for downsampling is used. In the right-hand-side path upsampling is done using the corresponding feature-maps generated followed by 2x2 convolution layers with cropping.

$$\mathbf{S_n(x) =exp(f_m(x))/\sum_{j=1}^{k} \binom{n}{k} Ʊ^{k} fm^{n-k}} \quad \text{- Eqn(5)}$$

The SoftMax Activation function is defined as $S_n(x)$ as in equation(5), Where f_m represents the activation function of Feature Map *j* at the pixel position $Ʊ \in \boldsymbol{ς}$ and $\boldsymbol{ς} \subset Ɽ^2$ x $Ɽ^2$.

In our proposed NeuroSegNet model supports pre-autocomputation of weights based on deferring pixel frequencies in trained data sets according to various classes, the NeuroSegNet is trained to identify separation borders.

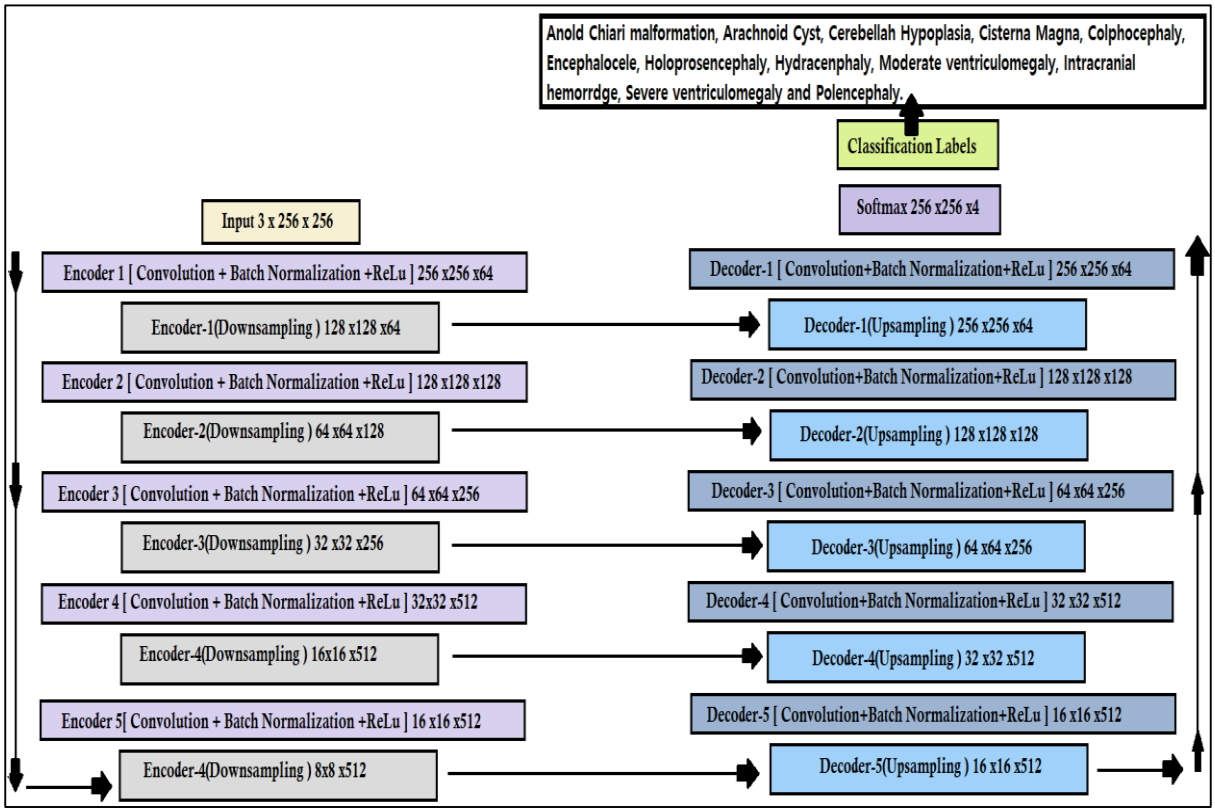

Figure -7 U-NeuroSegNet Processing

The morphological operation in U-Net is modified in U- NeuroSegNet using the separation borders as shown in equation (6).

$$GƆ(i)=GƆ_c(i)+GƆ_0.\log\frac{1}{2\eta}\oint-\frac{[\Re 1(X)-\Re 2(X)]2}{2\acute{w}}\delta z \quad \text{- Eqn(5)}$$

Where GƆ(x) is the precomputation of weights, $GƆ_c$ represents weight map, η denotes the nodes in one neuron in NeuroSegNet, the value of ẃ=0.25 bias to best fit, δz=11.12, ℜ1denotes the distance to the nearest pixel's border of the malignment and ℜ2 represents the separation to the second closest pixels border.

4.4 Training and Optimization

The "Training and Optimization" module focuses on training the model, using brain medical image data to identify neurological conditions. It involves optimizing the models architecture and hyperparameters to improve performance.

4.4.1 Feature Scaling

In the context of the work done, which involves deep learning for panoptic segmentation in medical images, feature scaling refer to normalizing the pixel values in the images. This normalization ensures that the model is not biased towards features with larger scales to improve the model's capacity for accurate classification of new data as well enhancing the training process futher. Specifically, in medical imaging, feature scaling could involve scaling pixel intensity values to a range that is suitable between 0 and 1.

In training and optimization phase, the proposed U-NeuroSegNet model undergoes iterative refinement to effectively segment. This process involves minimizing a predefined loss function, typically tailored for panoptic segmentation tasks, which quantifies the disparity between the ground truth labels and the projected segmentation.

4.4.2 Predicted Mask

The predicted mask is a binary image that indicates the regions within the input image that the model has identified as instances of the neurological condition being targeted. Each pixel in the predicted mask is assigned a value of 1 if the model predicts that the pixel belongs to the neurological condition, and 0 otherwise.

Panoptic Segmentation's Instance Segmentation within the brain identify neurological abnormalities by delineation of individual abnormal instances within the segmented regions. This process is crucial for accurately characterizing the spatial extent and distribution of abnormalities within brain scan images. Techniques commonly employed for instance segmentation include connected component analysis and clustering.

Connected component analysis identifies contiguous regions within the segmented tumor mask, assigning a unique label to each connected region representing an individual abnormality instance. Clustering algorithms can also be utilized to partition the segmented regions into distinct clusters, each corresponding to a separate tumor instance.

Integration is the subsequent step that combines the segmented tumor instances with relevant clinical data to provide a comprehensive understanding of tumor characteristics. This integration process facilitates the correlation of image findings with clinical parameters such as patient demographics, histopathological data, and treatment history. By amalgamating image-derived features with clinical insights, the system can offer more nuanced and informed interpretations of neurological abnormalties behavior and progression. This integrated approach aids healthcare professionals in making more accurate diagnoses, devising tailored treatment plans, and monitoring the effectiveness of interventions. Thus, Instance Segmentation and Integration synergistically contribute to enhancing the clinical utility of the abnormal neurological disease detection system.

4.4.3 Inference Engine Deployment

Inference engine deployment refers to the process of deploying NeuroSegNet for making predictions or inferences on new data. In the process of deploying inference engine involves preparing the model to be used in a production environment, such as a healthcare facility, where it can analyze brain scan images and identify neurological conditions.

The final step in the Neurological Abnormalities Detection System is the Inference Engine Deployment, where the trained model is used for inference in real time on fresh medical images. This pivotal module ensures that the system seamlessly integrates into existing healthcare infrastructure, facilitating its adoption and usage in clinical settings.

One of the primary objectives of Inference Engine Deployment is to optimize computational efficiency. This involves ensuring that the deployed model can efficiently process incoming medical images within acceptable timeframes, enabling prompt diagnosis techniques such as model optimization, hardware acceleration, and parallel processing may be employed to enhance computational speed and efficiency.

Scalability is another crucial aspect addressed by this module. As the system encounters increasing volumes of medical image data, it is capable of handling the workload without compromising performance. Inference Engine Deployment ensures that the deployed model can scale effectively to accommodate growing demands, through distributed computing architectures.

Inference Engine Deployment involves estimating the time required for processing a batch of images using the deployed model. The formula calculates the total inference time by multiplying the number of images to be processed (Б) with the average processing time per image (ꝑꝑ), and then dividing by the number of GPUs (§) utilized for parallel processing.

$$T = Б * ꝑꝑ / § \quad \text{- Eqn(7)}$$

T: Specifies the Inference Time Representing the time taken for inference in seconds.
Б: Denotes the number of images to be processed.
ꝑꝑ: Signifies the average processing time per image in seconds.
§: Represents the number of GPUs utilized for parallel processing during inference.

4.5.4 Ground Truth

The manually created mask in a medical image that shows the true areas affected by a neurological condition is called the ground truth. This ground truth mask carefully outline the areas in the image that correspond to the presence of the neurological condition. Each pixel in the ground truth mask is assigned a value of 1 if it belongs to the neurological condition and 0 otherwise. The ground truth mask, which is the original manually annotated mask that shows the actual regions of the neurological condition in the image, is compared to the current predicted mask. This comparison allows you to evaluate the performance of NeuroSegNet's accuracy.

5. RESULTS AND DISCUSSION

The NeuroSegNet developed in the study yielded promising and effective results in predicting various types of abnormal neurological conditions. The below figure 8 and 9 showcases the sample training and valid prediction batches.

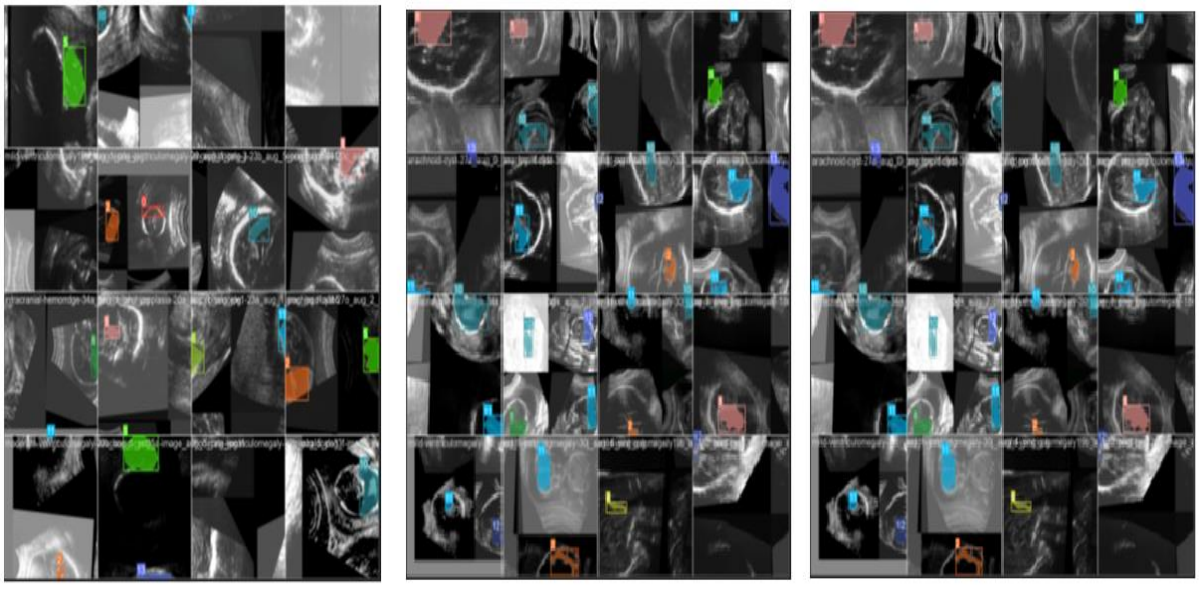

Figure 8 - Representation of Training Batches

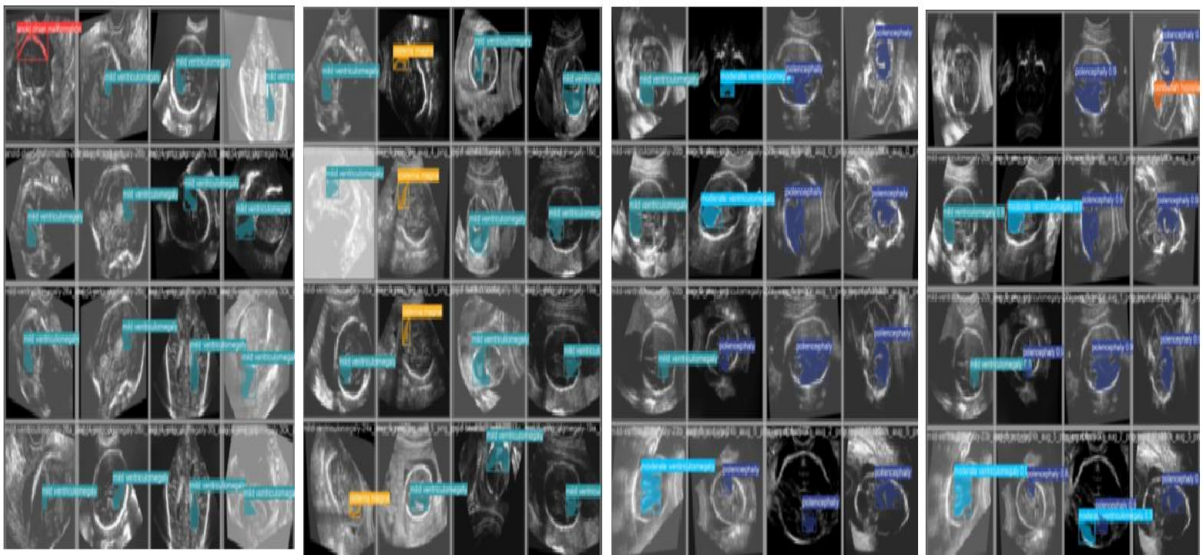

Figure 9 - Representation of Valid Prediction Batches

The below Figure 11 shows the results of the designed multiclass NeuroSegNet model for various Neurological Conditions. Our Proposed work is a deep learning-based neuro panoptic segmentation object detection approach which processes and diagnose big sets brain scan images to find neurological abnormalities like Anold Chiari malformation, Arachnoid Cyst, Cerebellah Hypoplasia, Cisterna Magna, Colphocephaly, Encephalocele, Holoprosencephaly, Hydracenphaly, Intracranial hemorrdge, mild/moderate/Severe ventriculomegaly and Polencephaly. We have achieved an overall accuracy of 98.2%.

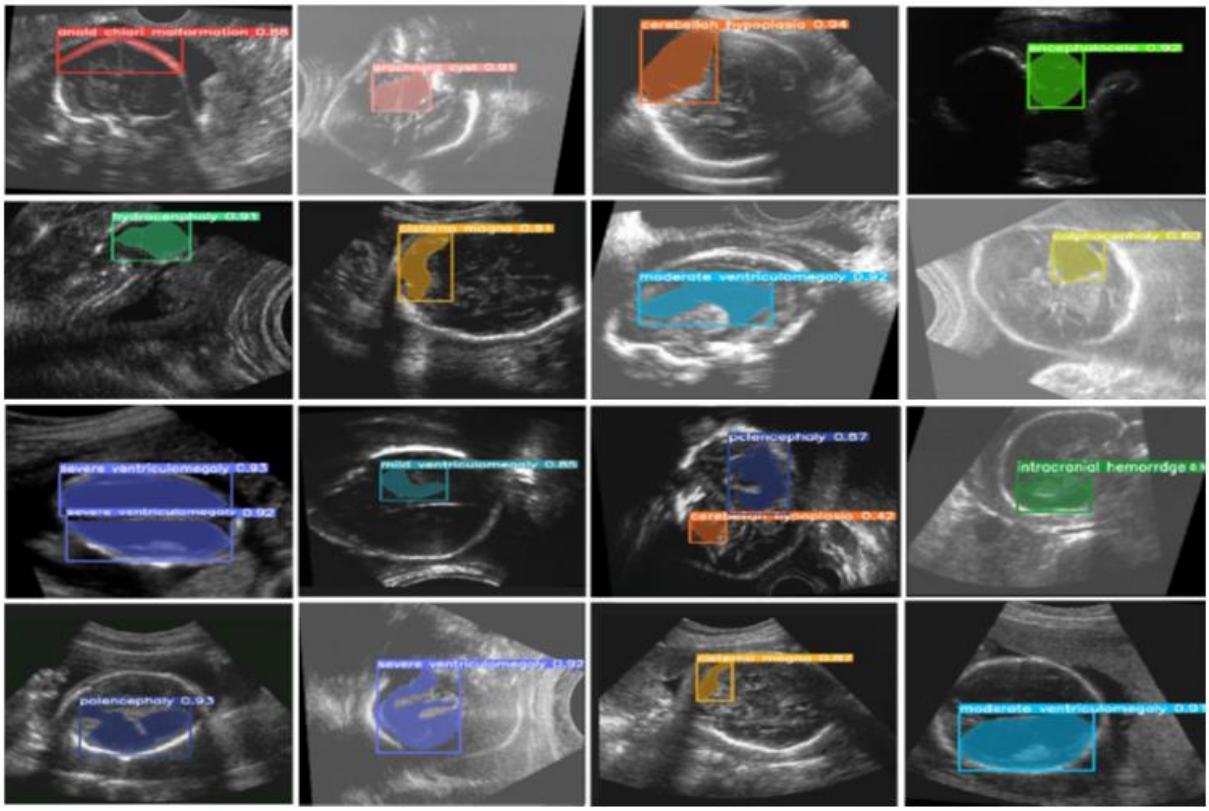

Figure 10 - Multiclass U-NeuroSegNet Prediction for various Neurological Conditions

The plotting of precision-confidence curve depicts the achieved precision value against various confidence thresholds for all classes. It serves as a vital metric showcasing the model's precision at different confidence levels. All Classes Anold Chiari malformation, Arachnoid Cyst, Cerebellah Hypoplasia, Cisterna Magna, Colphocephaly, Encephalocele, Holoprosencephaly, Hydracenphaly, Intracranial Hemorrdge, Mild/Moderate/Severe Ventriculomegaly and Polencephaly. Our model shows high level of precision of 95% as shown in figure 11. A precision score of 1.00 indicates that the U-NeuroSegNet did not make any false-positive predictions.

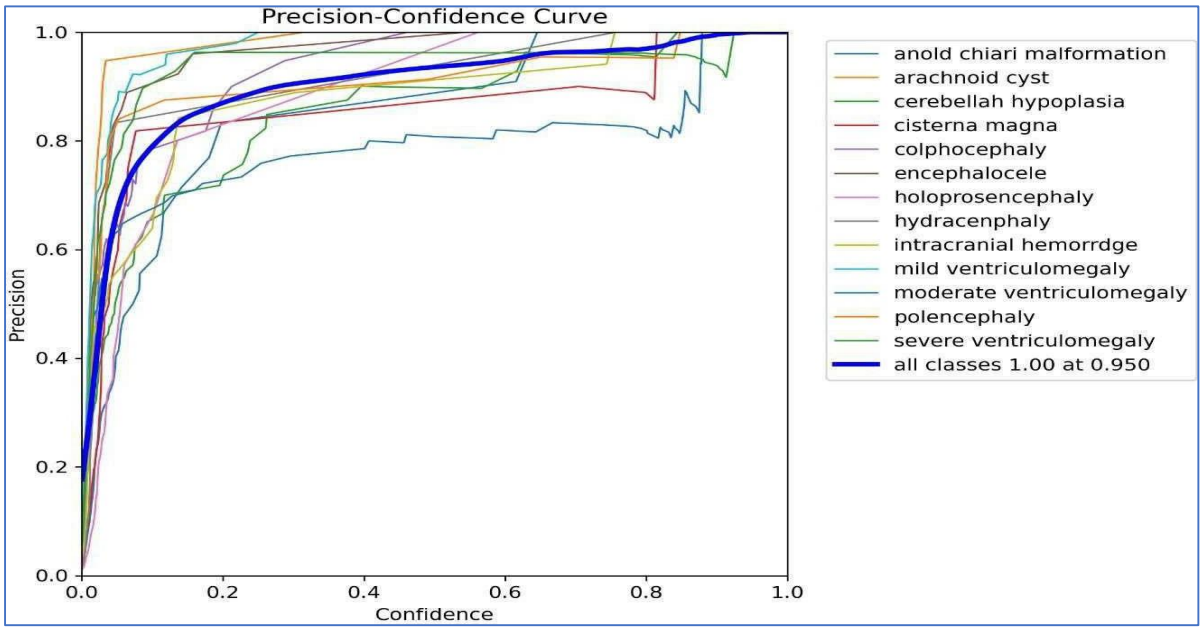

Figure 11 - Precision-Confidence Curve of The Model Over the Classes

The Recall-Confidence Curve plot for all classes is shown below. The curve illustrates the recall achieved against several threshold values of confidence. All classes 0.98 at 0.00 means that all classes exhibited recall rate of 98% based on true positives results as the graph-plot represents in figure 12.

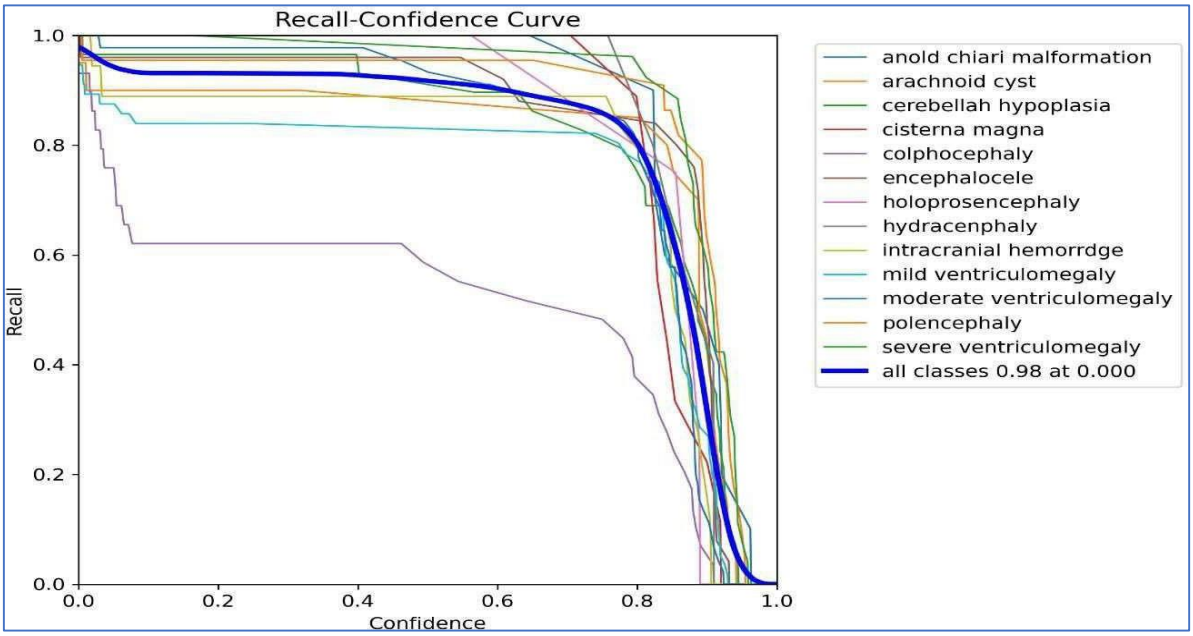

Figure 12 - Recall-Confidence Curve of The Model Over the Classes

The trade-off between recall and precision across a range of confidence thresholds is displayed by the Precision-Recall curve. Every class is showing 0.944 mAP@0.5. Figure 13 illustrates that the proposed U-NeuroSegNet's precision at Intersection over Union (IoU) in ground truth at 0.5 threshold is 94.4.

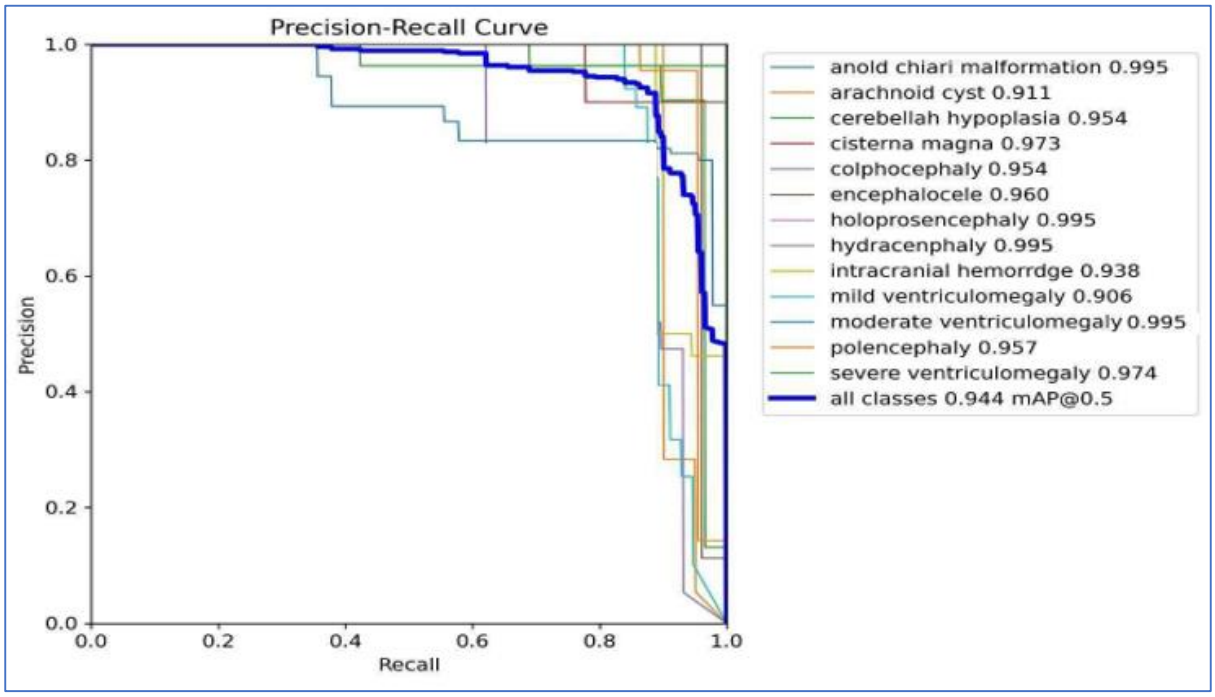

Figure 13 – The U-NeuroSegNet model's Precision-Recall Curve over the Classes

The below graph shows confusion matrix depicting the performance of Anold Chiari malformation, Arachnoid Cyst, Cerebellah Hypoplasia, Cisterna Magna, Colphocephaly, Encephalocele, Holoprosencephaly, Hydracenphaly, Intracranial Hemorrdge, Severe Ventriculomegaly and Polencephaly classes.The diagonal value of classes illustrates the correct classification and off diagonal values indicates wrong classification done. The overall classification performance across all classes is 98.2%, as illustrated in Figure 14.

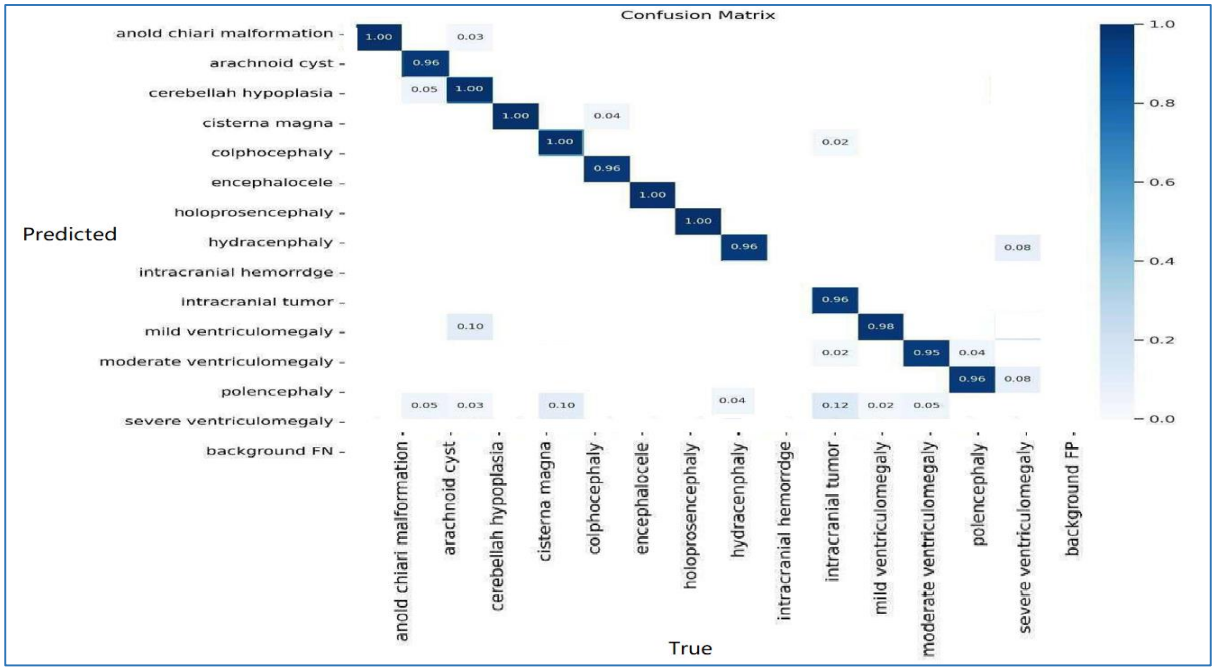

Figure 14 - performance across various labels using Confusion Matrix

To quantify losses in the training data, the metrics Classification_Loss , Object_Loss, Segmentation_loss and Box_loss were used to evaluate the NeuroSegNet model. In this model, the performance of the deep NIWatershed algorithm over the training data is found to be optimal. In the proposed deep NeuroSegNet model, the training loss over dataset is typically measured after each iteration. The validation loss is measured over fresh, unknown data, while the training loss indicates how well the model performs, or how well it fits the trained data. Figure 15 illustrates very low to negligible loss our model experienced for all classes.

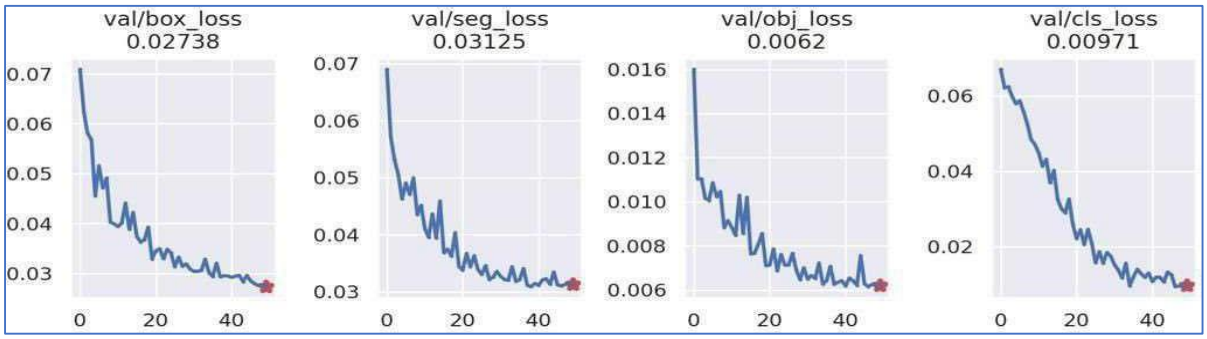

Figure 15 - Train dataset over Loss functions

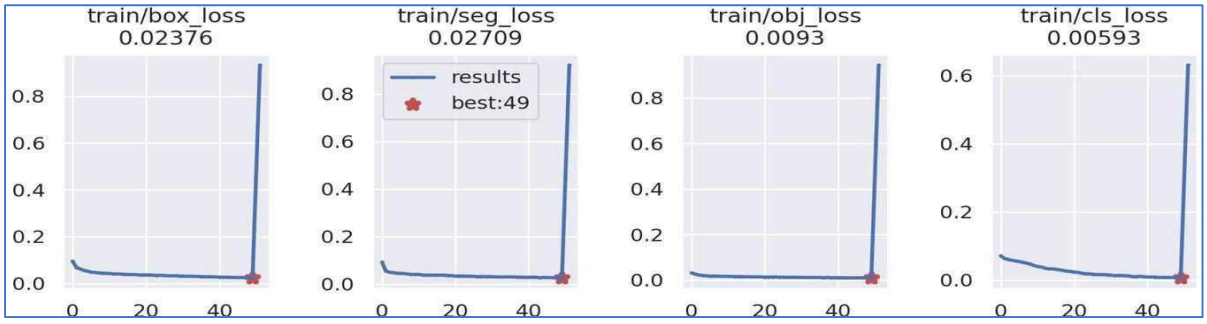

Figure 16 - Validation dataset over Loss function

In our NeuroSegNet model a standard indicator Mean average precision was used to measure the object detection algorithms' accuracy. The plots shown below displays the mean average precision for object detection across all classes @mAP0.5. The sub-metrics used to measure the Mean Average Precision (mAP) in our NeuroSegNet model includes the Confusion Matrix, Union of Intersection in segmented regions, Recall and Precision. The performance of our proposed model evaluated yielded 97.3 over mAP for an average set of queries.

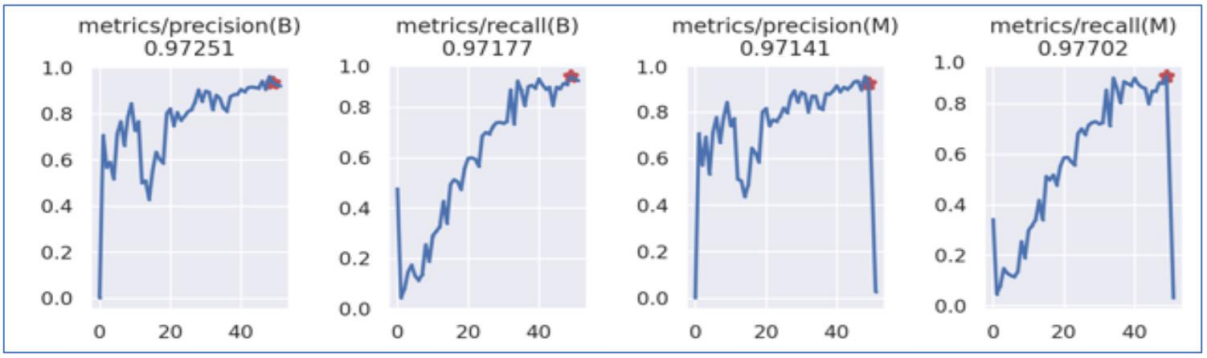

Figure 17 -Metrics over Recall, Precision and Mean Average Precision

Table -2 PERFORMANCE EVALUATION OF VARIOUS METRICS

METRICS/ AUTHORS	R-CNN	Mask-R-CNN	MSCA UNet	3DUNet	VGG-16	NEUROSEGNET
TRAINING IMAGE	1000	800	1200	1500	900	1800
TESTING IMAGE	300	200	400	250	350	500
SPLITTING RATIO	70:30	80:20	75:25	60:40	65:35	70:30
TESTING ACCURACY	85%	87%	84%	88%	83%	94%
OPTIMIZER	Adam	SGD	SGD	Adam	Adam	RMSProp
ALGORITHM	VGGNet	ResNet	MobileNet	LeNet	AlexNet	Watershed
FINAL LAYER ACTIVATION METHOD	Sigmoid	ReLU	Tanh	Sigmoid	ReLU	Softmax
SPECIFICITY	0.85	0.88	0.82	0.86	0.83	0.95
F-SCORE	0.88	0.89	0.87	0.90	0.86	0.95
SENSITIVITY	0.90	0.92	0.88	0.91	0.89	0.94
LOSS	5%	4%	6%	3%	5%	2%
SPEED	30 sec	25 sec	35 sec	40 sec	28 sec	20 sec
EVALUATION OF THE MODEL	77.81	90.11	62.74	88.52	77.98	96.81
PRECISION	87	89	86	90	85	97
ACCURACY	0.88	0.90	0.87	0.91	0.86	0.98

The performance metrics of our model, which includes F-score, sensitivity, precision, accuracy, and testing accuracy, exceed those of all previous works. This indicates the superior capability of our model to accurately detect and classify abnormal neurological conditions.

Additionally, our proposed work employs the RMSProp optimizer, known for its effectiveness in optimizing deep learning models. For binary classification tasks, the final layer's use of the Softmax activation function guarantees proper output scaling. Moreover, the model evaluation demonstrates a low error rate of only 1.8%, indicating the robustness of our model in minimizing classification errors.

CONCLUSION AND FUTURE WORK

NeuroSegNet was designed based on panoptic segmentation to identify abnormal neurological condition using medical images. The developed model was run over big data apache spark GPU based environment. In Spark clusters, the yolo files are placed in its data center folder. This model can identify thirteen types neurological conditions. Earlier research works only focused on one class like Anold Chiari malformation and Ventriculomegaly but in our work we developed a model that can detect

thirteen types for neurodegenerative disorders. The model gives accurate results for large datasets and at good speed. By streamlining the workflow of healthcare professionals and facilitating early detection, it ultimately contributes to improved patient care and outcomes. The system developed is highly efficient and robust, resulting in quicker and more precise identification and segmentation of degenerative neurological anomalies in medical images. By integrating real-time or near-real-time processing capabilities, the system significantly accelerates the diagnostic workflow, allowing healthcare professionals to make informed decisions more swiftly.

The work on brain neurological abnormalities classification based on neuro oncology, is a powerful tool The system's high performance in rigorous evaluation and validation studies underscores its reliability and utility in clinical practice. In order to ensure the system's seamless integration into appropriate clinical workflows and its widespread adoption by healthcare professionals, ongoing efforts to refine and optimize it are vital.

By combining technological innovation with practical application, this NeuroSegNet model stands as a pivotal tool in improving advanced medical imaging procedures and the general standard of neurology care.

The potential of our model is huge for changing the way brain imaging is used in diagnosing and treating neurological diseases. Our future plans include expanding our class offerings to serve as a comprehensive model for diagnosing neurological disorders. In the future there is lot of scope for improvement in model optimization, hardware acceleration, parallel processing and may be employed to further enhance computational speed and efficiency.

REFERENCES

[1] Yang, R., & Yu, Y., (2023). Artificial convolutional neural network in object detection and semantic segmentation for medical imaging analysis. Frontiers in oncology, 11, 638182.

[2] Elyan, E., Vuttipittayamongkol, P., Johnston, P., Martin, K., McPherson, K., Jayne, C., & Sarker,M. K (2023). Computer vision and machine learning for medical image analysis: recent advances, challenges, and way forward. Artificial Intelligence Surgery.

[3] Chen, X., Wang, X., Zhang, K., Fung, K. M., Thai, T. C., Moore, K., Qiu, Y., (2022). Recent advances and clinical applications of deep learning in medical image analysis. Medical Image Analysis, 79, 102444.

[4] Yu, H., Yang, L. T., Zhang, Q., Armstrong, D., & Deen, M. J., (2023). Convolutional neural networks for medical image analysis: state-of-the-art, comparisons, improvement and perspectives. Neurocomputing, 444, 92-110.

[5] Chen, J., Yang, N., Zhou, M., Zhang, Z., & Yang, X., (2022). A configurable deep learning framework for medical image analysis. Neural Computing and Applications, 34(10), 7375- 7392.

[6] Yao, X, Wang, X., Wang, S. H., Zhang, Y. D, (2020). A comprehensive survey on convolutional neural network in medical image analysis. Multimedia Tools and Applications,1-45

[7] Abdou, M. A, (2022). Literature review: Efficient deep neural networks techniques for medical image analysis. Neural Computing and Applications, 34(8), 5791-5812.

[8] Qian, L , Qian,W , Tian,T , Zhu,Y , Zhao,H, And Yao,Y, (2023). MSCA-UNet: Multi-Scale Convolutional Attention UNet for Automatic Cell Counting Using Density Regression, Digital Object Identifier 10.1109/ACCESS.2023.3304993.

[9] Yang, R., Yu, J., Yin, J., Liu, K., & Xu, S., (2023). A dense R-CNN multi-target instance segmentation model and its application in medical image processing. IET Image Processing, 2495.

[10] Kainz, P., Pfeiffer, M., Urschler, M., (2023). Semantic segmentation of colon glands with deep convolutional neural networks and total variation segmentation.

[11] M. Shettar, R. Karkal, R. Misra, A. Kakunje, V.V.M. Chandran, R.D. Mendonsa (2018).

Arachnoid cyst causing depression and neuropsychiatric symptoms: a case report East Asia. Arch. Psychiatry Off. J. Hong Kong Coll. Psychiatrist. Dong Ya Jing Shen Ke Xue Zhi Xianggang Jing Shen Ke Yi Xue Yuan Qi Kan, 28 pp. 64-67

[12] Hoogi, A., Subramaniam, A., Veerapaneni, R., Rubin, D., (2023). Adaptive estimation of active contour parameters using convolutional neural networks and texture analysis. IEEE Trans Med Imaging.

[13] Wolterink, J. M., Leiner, T., de Vos, B. D., van Hamersvelt, R. W., Viergever, M. A., Isgum, I., (2022). Automatic coronary artery calcium scoring in cardiac CT angiography using paired convolutional neural networks. Med Image Anal 34, 123– 136.

[14] Worrall, D. E., Wilson, C. M., Brostow, G. J., (2022). Automated retinopathy of prematurity case detection with convolutional neural networks. In:LMIA. Vol. 10008 of Lect Notes Comput Sci. pp. 68–76.

[15] Wu, A., Xu, Z., Gao, M., Buty, M., Mollura, D. J., (2022). Deep vessel tracking: A generalized probabilistic approach via deep learning. In: IEEE Int Symp Biomedical Imaging. pp. 1363–1367.

[16] Veta, M., van Diest, P. J., Pluim, J. P. W., (2022). Cutting out the middleman: measuring nuclear area in histopathology slides without segmentation. In: Med Image Comput Assist Interv. Vol. 9901 of Lect Notes Comput Sci. pp. 632–639.

[17] Vincent, P., Larochelle, H., Lajoie, I., Bengio, Y., Manzagol, P.-A., (2022). Stacked denoising autoencoders: Learning useful representations in a deep network with a local denoising criterion. J Mach Learn Res 11.

[18] Yang, D., Zhang, S., Yan, Z., Tan, C., Li, K., Metaxas, D., (2022). Automated anatomical landmark detection on distal femur surface using convolutional neural network. In: IEEE Int Symp Biomedical Imaging.

[19] Xie, Y., Xing, F., Kong, X., Su, H., Yang, L., (2021). Beyond classification: Structured regression for robust cell detection using convolutional neural network. In: Med Image Comput Assist Interv. Vol. 9351 of Lect Notes Comput Sci. pp. 358–365.

[20] Vincent, P., Larochelle, H., Lajoie, I., Bengio, Y., Manzagol, P.A., (2021). Stacked denoising autoencoders: Learning useful represen tations in a deep network with a local denoising criterion. J Mach Learn Res 11, 3371–3408.

[21] Xie, Y., Xing, F., Kong, X., Su, H., Yang, L., (2021). Beyond classification: Structured regression for robust cell detection using convolutional neural network. In: Med Image Comput Assist Interv. Vol. 9351 of Lect Notes Comput Sci. pp. 358–365.

[22] Xing, F., Xie, Y., Yang, L., (2021). An automatic learning-based framework for robust nucleus segmentation. IEEE Trans Med Imaging 35 (2), 550–566.

[23] F. Isensee et al. (2020). U-Net for brain tumor segmentation, International MICCAI Brain lesion Workshop, pp. 118-132,2020.

[24] Z. Jiang et al., (2021). Brain tumor segmentation in multi-parametric magnetic resonance imaging using model ensembling and super-resolution, International MICCAI Brain lesion Workshop, pp. 125-137, 2021.

[25] S. Thakur et al.,(2020). Brain extraction on MRI scans in presence of diffuse glioma: multi- institutional performance evaluation of deep learning methods and robust modality-agnostic training, NeuroImage, 2020.

[26] S. Bakas, H. Akbari, A. Sotiras, M. Bilello, M. Rozycki, J.S. Kirby, J.B. Freymann, K. Farahani, C. Davatzikos (2018). Advancing the cancer genome atlas glioma MRI collections with expert segmentation labels and radiomic features, 2018.

[27] Yuadi, I., Nihaya, U., & Pratiwi, F. D. (2023). Watershed Segmentation for Printed Source Classification. In Proceedings - IEIT 2023: 2023 International Conference on Electrical and Information Technology (pp. 275-280). (Proceedings - IEIT 2023: 2023 International Conference on Electrical and Information Technology). Institute of Electrical and Electronics Engineers Inc.. https://doi.org/10.1109/IEIT59852.2023.10335592

[28] S. Bakas, H. Akbari, A. Sotiras, M. Bilello, M. Rozycki, J. Kirby, J. Freymann, K. Farahani, C. Davatzikos (2018). Segmentation Labels and Radiomic Features for the Pre-operative Scans of the Tcga- Gbm Collection, 2018.

[29] Ö. Çiçek, A. Abdulkadir, S.S. Lienkamp, T. Brox, O. Ronneberger (2021). 3D U-Net: Learning Dense Volumetric Segmentation from Sparse Annotation, 2021.

[30] J. Doshi, G. Erus, M. Habes, C. Davatzikos(2019). DeepMRSeg: A Convolutional Deep Neural Network for Anatomy and Abnormality Segmentation on MR Images, arXiv E- Prints, 2019.

[31] M. Drozdzal, E. Vorontsov, G. Chartrand, S. Kadoury, C. Pal (2017). The Importance of Skip Connections in Biomedical Image Segmentation, 2017.

[32] H. Hwang, H.Z.U. Rehman, S. Lee (2020). 3D U-NET for skull stripping in brain MRI, https://www.mdpi.com/2076-3417/9/3/569.

[33] Fabian Isensee, Marianne Schell, Irada Pflueger, Gianluca Brugnara, David Bonekamp, Ulf Neuberger, Antje Wick, Heinz-Peter Schlemmer, Sabine Heiland, Wolfgang Wick, Martin Bendszus, Klaus H. Maier-Hein, Philipp Kickingereder (2021). Automated brain extraction of multisequence MRI using artificial neural networks,2021.

[34] M.M. Kim, H.A. Parmar, M.P. Aryal, C.S. Mayo, J.M. Balter, T.S. Lawrence, Y. Cao(2019).Developing a pipeline for multiparametric MRI-guided radiation therapy: initial results from a phase- II clinical trial in newly diagnosed glioblastoma, Tomography, 2019.

[35] J. Leote, R.G. Nunes, L. Cerqueira, R. Loução, H.A. Ferreira (2018). Reconstruction of white matter fiber tracts using diffusion kurtosis tensor imaging at 1.5t: pre-surgical planning in patients with glioma, 2018.

[36] J. Long, E. Shelhamer, T. Darrell(2016). Fully convolutional networks for semantic segmentation, 2016.

[37] M. J. Lakshmi and S. N. Rao (2022). Brain tumor magnetic resonance image classification: A deep learning approach", Soft Comput., vol. 26, no. 13, pp. 6245- 6253, Jul. 2022.

[38] T.N. Nadkarni, M.J. Andreoli, V.A. Nair, P. Yin, B.M. Young, B. Kundu, J. Pankratz, A. Radtke, R. Holdsworth, J.S. Kuo, A.S. Field, M.K. Baskaya, C.H. Moritz,M.E. Meyerand, V. Prabhakaran(2021). Usage of FMRI for pre-surgical planning in brain tumor and vascular lesion patients: task and statistical threshold effects on language lateralization, 2021.

[39] W. Jun and Z. Liyuan (2022). Brain tumor classification based on attention guided deep learning model, Int. J. Comput. Intell. Syst., vol. 15, no. 1, pp. 35, Dec. 2022.

[40] T. Fernando, H. Gammulle, S. Denman, S. Sridharan and C. Fookes (2022). Deep learning for medical anomaly detection—A survey, ACM Comput. Surveys, vol. 54, no. 7, pp. 1-37, Sep. 2022.

[41] A. S. Lundervold and A. Lundervold (2019). An overview of deep learning in medical imaging focusing on MRI, Zeitschrift für Medizinische Physik, vol. 29, no. 2, pp. 102-127, 2019.

[42] S. Bonte, I. Goethals and R. Van Holen(2020). Machine learning based brain tumour segmentation on limited data using local texture and abnormality, Comput. Biol. Med., vol. 98, pp. 39-47, Jul. 2018.

[43] L. Rundo, C. Militello, A. Tangherloni, G. Russo, S. Vitabile, M. C. Gilardi, et al.(2018). NeXt for neuro-radiosurgery: A fully automatic approach for necrosis extraction in brain tumor MRI using an unsupervised machine learning technique, Int. J. Imag. Syst. Technol., vol. 28, no. 1, pp.21-37, Mar. 2018.

[44] D. Liu, D. Zhang, Y. Song, F. Zhang, L. J. O'Donnell and W. Cai (2018). 3D large kernel anisotropic network for brain tumor segmentation, Proc. Int. Conf. Neural Inf. Process., pp. 444-454, 2018.

[45] M. W. Nadeem, M. A. A. Ghamdi, M. Hussain, M. A. Khan, K. M. Khan, S. H. Almotiri, et al(2020). Brain tumor analysis empowered with deep learning: A review taxonomy and future challenges, Brain Sci., vol. 10, no. 2, pp. 118-151, 2020.

[46] Y. Bhanothu, A. Kamalakannan, G. Rajamanickam (2020). Detection and classification of brain tumor in MRI images using deep convolutional network, Proc. 6th Int. Conf. Adv. Comput. Commun. Syst. (ICACCS), pp. 248-252, Mar. 2020.

[47] H. Mohsen, E.-S. A. El-Dahshan, E.-S. M. El-Horbaty,A.-B. M. Salem (2018).Classification using deep learning neural networks for brain tumors, Future , vol. 3, no. 1, pp. 68-71.

[48] J. S. Paul, A. J. Plassard, B. A. Landman , D. Fabbri (2017). Deep learning for brain tumor classification, Proc. SPIE, vol. 10137, pp. 1013710-1013726, 2017.

[49] C. N. Ladefoged, L. Marner, A. Hindsholm, I. Law, L. Højgaard and F. L. Andersen(2018). Deep learning-based attenuation correction of PET/MRI in pediatric brain tumor patients: Evaluation in a clinical setting, Frontiers Neurosci, vol. 2, pp. 1005.

[50] H. Fabelo, M. Halicek, S. Ortega, M. Shahedi, A. Szolna, J. Piñeiro, et al.(2019). Deep learning-based framework for in vivo identification of glioblastoma tumor using hyperspectral images of human brain, Sensors, vol. 19, no. 4, pp. 920, Feb. 2019.

[51] B. Amarapur (2020). Computer-aided diagnosis applied to MRI images of brain tumor using cognition based modified level set and optimized ANN classifier, Multimedia Tools Appl., vol. 3601, pp. 3571-3599, Feb. 2020.

[52] E. Benson, M. P. Pound, A. P. French, A. S. Jackson and T. P. Pridmore(2018). Deep hourglass for brain tumor segmentation, Proc. Int. MICCAI Brain lesion Workshop, vol. 10, no. 2, pp. 419-428, 2018.

[53] G. (2018). Brain tumor segmentation using deep fully convolutional neural networks in Brain lesion: Glioma, Multiple Sclerosis, Stroke and Traumatic Brain Injuries, Springer, vol. 10670, 2018.

[54] P. Afshar, A. Mohammadi and K. N. Plataniotis(2018). Brain tumor type classification via capsule networks, Proc. 25th IEEE Int. Conf. Image Process. (ICIP), pp. 3129- 3133, Oct. 2018.

[55] F. Isensee et al. (2017). Brain tumor segmentation using large receptive field deep convolutional neural networks, Bildverarbeitung für die Medizin 2017, Berlin, Germany:Springer Vieweg, 2021.

[56] S. Kumar, A. Negi and J. N. Singh(2019). Semantic segmentation using deep learning for brain tumor MRI via fully convolution neural networks, Information and Communication Technology for Intelligent Systems, Singapore:Springer, pp. 11-19, 2019.

[57] S. Deepak and P. M. Ameer (2019). Brain tumor classification using deep CNN features via transfer learning, Comput. Biol. Med., vol. 111, pp. 1-7, Aug. 2019.

[58] V. K. Deepak and R. Sarath(2022). An intelligent brain tumor segmentation using improved deep learning model based on cascade regression method, Multimedia Tools Appl., pp. 1-20, Dec. 2022.

[59] E. U. Haq, H. Jianjun, K. Li, H. U. Haq and T. Zhang(2021). An MRI-based deep learning approach for efficient classification of brain tumors, J. Ambient Intell. Humanized Comput., pp. 1-22, Oct. 2021.

[60] R. Ranjbarzadeh, A. B. Kasgari, S. J. Ghoushchi, S. Anari, M. Naseri and M. Bendechache(2021). Brain tumor segmentation based on deep learning and an attention mechanism using MRI multi- modalities brain images, Sci. Rep., vol. 11, no. 1, pp. 10930, May 2021.

[61] T. Ruba, R. Tamilselvi and M. P. Beham (2022). Brain tumor segmentation in multimodal MRI images using novel LSIS operator and deep learning, J. Ambient Intell. Humanized Comput., pp. 1- 15, Mar. 2022.

[62] A. Verma and V. P. Singh (2022). Design analysis and implementation of efficient deep learning frameworks for brain tumor classification, Multimedia Tools Appl., vol. 81, no. 26, pp. 37541- 37567, Nov. 2022.

[63] Gabriel. L,Nasim .H, Irene Cheng(2022). Semi-supervised learning approach for localization and pose estimation of texture-less objects in cluttered scenes, Volume 16,
December 2022, 100247.

[64] P. K. Ramtekkar, A. Pandey and M. K. Pawar (2022). Innovative brain tumor detection using optimized deep learning techniques, System Assurance Eng. Manage., vol.14, no.1, pp.459-473, Feb. 2022.

[65] Haddad FA, Qaisi I, Joudeh N, et al (2018). The newer classifications of the Chiari malformations with clarifications: an anatomical review. Clin Anat 2018; 31:314–22
doi:10.1002/ca.23051 pmid:29344999.

[66] Fons K, Jnah AJ (2021). Arnold-Chiari Malformation: Core Concepts. Neonatal Netw. 2021 Aug 01;40(5):313-320.

[67] Grasso G, Torregrossa F (2019). Minimally Invasive Surgery for Decompression in Chiari I Malformation. World Neurosurg. 2019 Aug; 128:333-335.

[68] Kotil K, Ozdogan S, Kayaci S, Duzkalir HG (2018). Long-Term Outcomes of a New Minimally Invasive Approach in Chiari Type 1 and 1.5 Malformations: Technical Note and Preliminary Results. World Neurosurg. 2018 Jul; 115:407-413.

[69] Quillo-Olvera J, Navarro-Ramírez R, Quillo-Olvera D, Quillo-Reséndiz J, Kim JS (2019). Minimally Invasive Craniocervical Decompression for Chiari 1 Malformation: An Operative Technique. J Neurol Surg A Cent Eur Neurosurg. 2019 Jul;80(4):312-317.

[70] James Kuhn; Luke J. Weisbrod; Prabhu D. Emmady (2024). Chiari Malformation Type 2, https://www.ncbi.nlm.nih.gov/books/NBK557498.

[71] Fritch, C., & Rizk, E. B. (2022). Arachnoid Cysts: an overview of concepts and review of the treatment literature. In Cerebrospinal Fluid and Subarachnoid Space: Pathology and Disorders, Volume 2 (pp. 1-6). Elsevier. https://doi.org/10.1016/B978-0-12-819507-9.00020-X

[72] Melo A., A.S. Santos A.S., A.S.dos Santos A.S. (2022). Psychotic symptoms associated with a frontoparietal arachnoid cyst: the role of neuroimaging studies in first-episode psychosis, Cureus, 14 (2022), p. e31652, 10.7759/cureus.31652

[73] Neesgaard V.E., Poulsen F.R., (2022). A.V. Holst, T.I. Mathiesen (2022). Arachnoid cysts can be associated with cognitive and affective symptoms, Ugeskrift Laeger, 184.

[74] Gjerde P.B., Litleskare S., Lura N.G., Tangen T., Helland C.A., Wester K., (2018).
Anxiety and depression in patients with intracranial arachnoid cysts–a prospective study
World Neurosurg., 132 (2019), pp. e645-e653, 10.1016/j.wneu.2019.08.058.

[75] Van Dijk .T, Baas .F, Barth .P.G, Poll-The .B.T (2018). What's new in pontocerebellar hypoplasia? An update on genes and subtypes. Orphanet J Rare Dis.;13(1):92.

[76] Nuovo. S, Micalizzi. A, Romaniello. R, Arrigoni. F, Ginevrino .M, Casella. A, (2022). Refining the mutational spectrum and gene-phenotype correlates in pontocerebellar hypoplasia: results of a multicentric study. J Med Genet;59(4):399–409.

[77] Morisaki .I, Shiraishi .H, Fujinami .H, Shimizu .N, Hikida .T, Arai .Y (2021). Modeling a human CLP1 mutation in mouse identifies an accumulation of tyrosine pre-tRNA fragments causing pontocerebellar hypoplasia type 10. Biochem Biophys Res Commun. 2; 570:60–6

[78] Appelhof .B, Wagner .M, Hoefele .J, Heinze .A, Roser .T, Koch-Hogrebe .M, et al (2021). Pontocerebellar hypoplasia due to bi-allelic variants in MINPP1. Eur J Hum Genet. 2021;29(3):411–21.

[79] Koray. S, Mekin. S, (2022). Reference ranges of fetal cisterna magna volume measurements by three-dimensional ultrasonography in the late second trimester considering sonographic experience,Volume 64, Issue 3,https://doi.org/10.1177/02841851221098846

[80] Yazici1.E, Kose. S, Gunduz Y, Kurt. E.M, Yazici. A. B, (2022). Mega cisterna magna in bipolar mood disorder: a case report,Page Path J Yeungnam Med Sci , Volume 39(1).

[81] Desdicioğlu .R,Ipek.A, Desdicioglu .K, Gumus .M, Yavuz .A.Y,(2021).Nomogram of Fetal Cisterna Magna Width in the Second Trimester of Pregnancy,Cyprus Journal of Medical Sciences 6(3):217-221,DOI: 10.5152/cjms.2021.1157.

[82] Kosky. K.M, Phenis. R, Kiselica. A.M, (2022). Neuropsychological functioning in dysgenesis of the corpus callosum with colpocephaly,Appl Neuropsychol Adult, 29 (2022), pp. 1681-1687,10.1080/23279095.2021.1897008.

[83] Reiter. K, Rothenberg. K.G, (2020). Neuropsychological presentation of colpocephaly and porencephaly with symptom onset in adulthood,Neurocase, 26 (6) 2020, pp. 353-359, 10.1080/13554794.2020.1841798.

[84] Parker .C, W Eilbert, T Meehan, C Colbert, (2019). Colpocephaly diagnosed in a neurologically normal adult in the Emergency Department,Clin Pract Cases Emerg Med, 3(4) (2019), pp. 421-424, 10.5811/cpcem.2019.9.44646.

[85] Durmaz Ö, Fatihoğlu E, Gülmez AO, (2022). Magnetic resonance measurement of lateral ventricular diameters in cases of colpocephaly and corpus callosum agenesis,Curr Res MRI, 1 (3) 2022, pp. 79-81, 10.5152/CurrResMRI.2022.222546.

[86] Rehman. G, Farooq, I. Bukhari (2018), Neurosurgical interventions for occipital Encephalocele, Asian J. Neurosurg., 13 (2), pp. 233-237.

[87] N.L. Pal, A.S. Juwarkar, S. Viswamitra (2021), Encephalocele: know it to deal with it
Egypt. J. Radiol. Nucl. Med., 52 (1).

[88] N. Apostolou, D. Gräfe, M. Knüpfer, M. Krause (2023), Managing an open nasofrontal encephalocele after birth Child's Nerv .Syst. [internet]., 39 (2) 2023, pp. 535-540,Available from: 10.1007/s00381-022-05620-6

[89] M. Arifin, W. Suryaningtyas, A.H. Bajamal (2018), Frontoethmoidal encephalocele: clinical presentation, diagnosis, treatment, and complications in 400 cases, Child's Nerv. Syst., 34 (6) (2018), pp. 1161-1168

[90] Y.A. Kousa, A.J. du Plessis, G. Vezina (2018), Prenatal diagnosis of holoprosencephaly, Am J Med Genet C Semin, Med Genet, 178 (2018), pp. 206-213

[91] Fedou. W, Mouna .H, Hasana. S, Boufettal .H, Mahdaoui. S, Samouh.N (2023). Holoprosencephaly (HPE) : case report and review of the literature, International Journal of Surgery Case Reports, Volume 110, September 2023,108723,https://doi.org/10.1016/j.ijscr.2023.108723

[92] Jiménez J.H., Galloc D., Pachajoab .H, Carrilloa E.F., Cifuentesc. R, Valderramaa A.,(2016).Prenatal diagnosis of trisomy 21 and semilobar holoprosencephaly. Presentation of a rare association,Revista Médica Internacional sobre el Síndrome de Down (English Edition),DOI: 10.1016/j.sdeng.2015.10.002

[93] Márquez I. G, Navarro L. F, Sánchez E.M (2022). The diagnosis of the middle interhemispheric variant ofholoprosencephaly with fetal MRI,Radiología (English Edition),Vol. 64. Issue 4. Pages 375-378.

[94] Omoto T, Takahashi T, Fujimori K, Kin S, (2020). Prenatal diagnosis of fetal microhydranencephaly: a case report and literature review Pregnancy Childbirth. 2020 Nov 11;20(1):688. doi: 10.1186/s12884-020-03400-1.PMID: 33176733.

[95] Sen K, Kaur S, Stockton DW, Nyhuis M, Roberson J, (2021). Biallelic Variants in LAMB1 Causing Hydranencephaly: A Severe Phenotype of a Rare Malformative Encephalopathy, AJP Rep. 2021 Jan;11(1):e26-e28. doi: 10.1055/s-0040-1722728. Epub 2021 Feb 1.PMID: 33542858.

[96] Kpélao E, Ahanogbé KMH, Egu K, Doléagbénou AK, Moumouni AEK, Sossoukpe S, Ségbédji KK, Bakondé HE, Lawson D, Abaltou B, Abdoulaye HM, Békéti KA, (2022). Children hydrocephalus in Togo: etiologies, treatment, and outcomes,Surg Neurol Int. 2022 Dec 2;13:560. doi: 10.25259/SNI_927_2022. eCollection 2022, PMID: 36600766.

[97] Egger .C, Dédouit .F, Schrag .B, Hanquinet .S, Fracasso .T,(2023).A forensic case of hydranencephaly in a preterm neonate fully documented by postmortem imaging techniques,Forensic Sci Res. 2023 Jan 13;8(1):79-83. doi: 10.1093/fsr/owad002.

eCollection 2023 Mar.PMID: 37415801.

[98] Hirata. W, Shinojima. T, Yokota. K, Kin. R, Yamada. T, Asakura .H, (2024).A case of testicular cancer in a long-term hydranencephaly survivor with undescended testes,IJU Case Rep. 2024 Apr 1;7(3):266-269. doi: 10.1002/iju5.12720. eCollection 2024 May,PMID: 38686073.

[99] Jafarzade A, Mungan T, Biri A (2023). Prenatal neuro ultrasound and fetal MRI conformity in ventriculomegaly. Actual Gyn. 2023;15:16-20.

[101] D'Addario, V, (2022). Diagnostic approach to fetal ventriculomegaly,Aus der Zeitschrift Journal of Perinatal Medicine https://doi.org/10.1515/jpm-2022-0312.

[102] J.H. Gilmore et al (2023). Outcome in children with fetal mild ventriculomegaly: a case series,Schizophrenia Research 48 (2001) 219-226.

[103]Fox NS, Monteagudo A, Kuller JA, Craigo S, Norton ME (2018).Mild fetal ventriculomegaly: diagnosis, evaluation, and management. Society for Maternal-Fetal Medicine, Am J Obstet Gynecol. 2018;219:0–9.

[104]Mary E. Norton, MD Nathan S. Fox, MD (2020).Fetal Ventriculomegaly,Society for Maternal-Fetal Medicine (SMFM),https://doi.org/10.1016/j.ajog.2020.08.182.

[105] Feng .X, Li .X, Jie Feng .J, Xia .J (2023).Intracranial hemorrhage management in the multi-omics era, Heliyon, Volume 9, Issue 3, March 2023, e14749.https://doi.org/10.1016/j.heliyon.2023.e14749.

[106] K. Shi, D.C. Tian, Z.G. Li, et al, (2019). Global brain inflammation in stroke,Lancet Neurol., 18 (11) (2019), pp.1058-1066, 10.1016/s1474-4422(19)30078.

[107] A.R. Saand, F. Yu, J. Chen, et al,(2019). Systemic inflammation in hemorrhagic strokes - a novel neurological sign and therapeutic target?J. Cerebr. Blood Flow Metabol., 39 (6) (2019), pp. 959-988,10.1177/0271678x19841443.

[108] N. Madangarli, F. Bonsack, R. Dasari, et al.(2019).Intracerebral hemorrhage: blood components and neurotoxicity Brain Sci., 9 (11),10.3390/brainsci9110316.

[109] M. Zulfiqar, F. Queadan, A. Ikram, M. Farooqui, S.P. Richardson, C.S. Calder, et al (2019).Intracerebral haemorrhage in multiple sclerosis: a retrospective cohort study.J Stroke Cerebrovasc Dis, 28 (2019), pp. 267-275.

[110] Ahmed S N, P Prakasam (2023). A systematic review on intracranial aneurysm and hemorrhage detection using machine learning and deep learning techniques,Prog Biophys Mol Biol , Oct:183:1-16. doi: 10.1016/j.pbiomolbio.2023.07.001. Epub 2023 Jul 25.

[111] Tambuzzi S, Gentile G, Zoja R (2022).Porencephalic cyst in adult, Autops Case Rep. 2022 Jan 7;12:e2021351. doi: 10.4322/acr.2021.351. eCollection 2022. PMID: 35350817.

[112] Dominguez JF, Shah S, Li B, Feldstein E, Kim MG, Tobias ME (2021). Porencephalic cyst after endoscopic third ventriculostomy and Ommaya reservoir placement: case report and review of the literature. Childs Nerv Syst.2021 Sep;37(9):2917-2921. doi: 10.1007/s00381-021-05042-w. Epub 2021 Jan 13.PMID: 3344275.

[113] Wynne D, Jalil MFA, Dhillon R (2020). Endoscopic Fenestration of a Symptomatic Porencephalic Cyst in an Adult, World Neurosurg,2020 Sep:141:245-246. doi: 10.1016/j.wneu.2020.06.092. Epub 2020 Jun 20.

[114] Lu D, Tan J, Xu H (2024). Ventriculoperitoneal shunt for giant porencephaly: a case report and literature review, Front Surg. 2024 Apr 19;11:1389050. doi: 10.3389/fsurg.2024.1389050. eCollection 2024, PMID: 38708364.

[115] Y. Zhang et al (2021).Deep multimodal fusion for semantic image segmentation: a survey, Image Vis. Comput,2021.

[116] Q. Tang et al (2021).Attention-guided chained context aggregation for semantic segmentation, Image Vis. Comput,2021.

[117] K. Tong et al (2020). Recent advances in small object detection based on deep learning: a review, Image Vis. Comput.2020.

[118] Gu. W,Bai .S, Kong .L(2022). A review on 2D instance segmentation based on deep neural networks, https://doi.org/10.1016/j.imavis.2022.104401.

[119] J. Tan et al (2021).HCFS3D: hierarchical coupled feature selection network for 3D semantic and instance segmentation, Image Vis. Comput.2021.

[120] Zhou. J,Lu .Y, Tao .S, Cheng .X, Huang .C (2021).E-Res U-Net: An improved U-Net model for segmentation of muscle images, https://doi.org/10.1016/j.eswa.2021.115625.

[121] Zhou. Z, Siddiquee. MMR, Tajbakhsh. N, Liang. J (2018). Unet++: A nested u-net architecture for medical image segmentation ,10.1007/978-3-030-00889-5_1.

[122] Ma H, Zou Y, Liu PX (2021). MHSU-Net: A more versatile neural network for medical image segmentation, Comput Methods Programs Biomed, 2021 Sep; 208:106230. doi: 10.1016/j.cmpb.2021.106230. Epub 2021 Jun 6. PMID: 34148011.

[123] Chen S, Zou Y, Liu PX (2021). IBA-U-Net: Attentive BConvLSTM U-Net with Redesigned Inception for medical image segmentation. Comput Biol Med. 2021 Aug;135:104551. doi: 10.1016/j.compbiomed.2021.104551. Epub 2021 Jun 12.
PMID: 34157471

[124] Li P, Li Z, Wang Z, Li C, Wang M (2024).mResU-Net: multi-scale residual U-Net-based brain tumor segmentation from multimodal MRI.Med Biol Eng Comput. 2024 Mar;62(3):641-651. doi: 10.1007/s11517-023-02965-1. Epub 2023 Nov 19. PMID: 37981627 Review.

[125] Sharma .A.K, Nandal .A,Dhaka .A, Koundal .D, Bogatinoska .D.C, Alyami .H (2024).Enhanced Watershed Segmentation Algorithm-BasedModified ResNet50 Model for Brain Tumor Detection,https://doi.org/10.1155/2022/7348344.